THE INVESTIGATION OF THE ROLE OF NF-κB IN THE PROLIFERATION AND DIFFERENTIATION OF HaCaT CELLS CONTAINING Cx26 KID SYNDROME MUTATIONS

A Thesis Submitted to
the Graduate School of
İzmir Institute of Technology
in Partial Fulfillment of the Requirement for the Degree of

MASTER OF SCIENCE

in Molecular Biology and Genetics

by
Ece İNAL

July 2024
İZMİR

We approve the thesis of **Ece İNAL**

Examining Committee Members

Assoc. Prof. Dr. Gülistan MEŞE ÖZÇİVİCİ
Department of Molecular Biology and Genetics,
İzmir Institute of Technology

Prof. Dr. Özden YALÇIN ÖZUYSAL
Department of Molecular Biology and Genetics,
İzmir Institute of Technology

Dr. Yavuz OKTAY
Basic and Translational Research Program,
İzmir Biomedicine and Genome Center

12 July 2024

Assoc. Prof. Dr. Gülistan MEŞE ÖZÇİVİCİ
Supervisor, Molecular Biology and Genetics,
İzmir Institute of Technology

Prof. Dr. Özden YALÇIN ÖZUYSAL
Head of the Molecular Biology and Genetics Program

Prof. Dr. Mehtap EANES
Dean of the Graduate School

ACKNOWLEDGEMENT

I express my sincere gratitude to my supervisor, Assoc. Prof. Dr. Gülistan Meşe ÖZÇİVİCİ for her guidance, patience, and kindness throughout this journey. Her expertise and insightful feedback have significantly contributed to the completion of this thesis and enhanced my academic development. I deeply appreciate her unwavering support from the very beginning of my research.

I am thankful to Prof. Dr. Engin ÖZÇİVİCİ and Prof. Dr. Özden YALÇIN ÖZUYSAL for their valuable comments and insights on this study.

I extend my heartfelt thanks to the members of my laboratory for their unwavering support. I would like to express my gratitude to Yağmur Ceren Ünal for her mentorship, which has significantly contributed to the development of my knowledge and skills. Special thanks to Sümeyye Şüheda Yaşarbaş, Meryem Azra Yıldırım, and Öykü Sarıgil for their support and friendships. I also wish to express my gratitude to Şüheda Özek, Yiğit Türközü, Ata Deniz Uzun, Halil İbrahim Erdol, and Batun Balcıoğlu who put great effort into this study.

I would like to thank Prof. Dr. Çağlar KARAKAYA for providing the Thermo ELECTRON CORPORATION Multiskan Spectrum. I am also grateful to Özgür Okvur and Dane Rusçuklu from IZTECH TAM CFB for their guidance with data analysis.

I express my deepest gratitude to my mother, Nazire İnal, my father, Ergün İnal, my brother, Ali Yiğit İnal, and my little sister, Nehir İnal, for their unwavering love and constant support throughout my life. I owe a debt of gratitude to Kahraman Eryeğit who has supported me since the day we met. I am deeply grateful to Aysu Kaya, Fatma Hacımalak, and Sena Konceli for their invaluable friendships.

I am grateful to The Scientific and Technological Research Council of Turkey (TÜBİTAK) for BİDEB 2210-A scholarship program, which supported me throughout this journey. This study is also funded by TÜBİTAK under grant number 119Z284.

To my dear family,

To all women in science…

ABSTRACT

THE INVESTIGATION OF THE ROLE OF NF-κB IN THE PROLIFERATION AND DIFFERENTIATION OF HaCaT CELLS CONTAINING Cx26 KID SYNDROME MUTATIONS

Keratitis-ichthyosis-deafness (KID) syndrome is a rare genetic disease characterized by deafness, visual impairments, and palmoplantar keratoderma. The disease arises from Connexin26 (Cx26) mutations that lead to the formation of hyperactive hemichannels causing uncontrolled molecule transfer across the membrane. Although the uncontrolled molecule transfer affects the proliferation and differentiation of keratinocytes, the exact molecular and cellular mechanisms underlying the epidermal alterations due to Cx26 mutations are not yet known. Previous studies showed enriched NF-κB pathway members in keratinocyte cell line HaCaT containing Cx26-D50Y KID syndrome mutation. Therefore, we hypothesized that Cx26 mutant channels may cause epidermal disorders by affecting keratinocyte proliferation and differentiation mechanisms via NF-kB pathway.

We investigated proliferation and differentiation mechanisms of the HaCaT cells that constitutively express the Cx26-G45E and Cx26-D50Y mutations, which cause different severity. G45E and D50Y containing cells showed the highest nuclear RelA and c-Rel signals, respectively. In addition, NaSal treatment affected early and late apoptosis rates differently in D50Y cells. Moreover, G45E and D50Y cells had opposite trends when early and late apoptosis rates were compared. Furthermore, NF-κB inhibition decreased proliferation rate of G45E cells, unlike WT cells. Lastly, cytokeratin10 protein levels showed differences in G45E cells after NaSal treatment.

NF-kB may affect apoptosis in KID syndrome mutants through distinct mechanisms and may have different effects on apoptosis mechanisms of D50Y. Furthermore, NF-kB may regulate proliferation and differentiation mechanisms of G45E. There is no available treatment for KID syndrome yet. Therefore, this study is important to understand the underlying mechanisms of KID syndrome.

ÖZET

Cx26 KID SENDROMU MUTASYONLARI İÇEREN HaCaT HÜCRELERİNİN PROLİFERASYONU VE FARKLILAŞMASINDA NF-κB'NİN ROLÜNÜN ARAŞTIRILMASI

Keratit-iktiyozis-sağırlık (KID) sendromu, Connexin26 (Cx26) mutasyonlarından kaynaklanan, sağırlık ve görme bozukluklarının yanı sıra palmoplantar keratoderma (avuç içi ve ayak tabanlarında epidermisin kalınlaşması) ile karakterize edilen nadir bir genetik hastalıktır. Cx26 mutasyonları, hücre zarında kontrolsüz molekül geçişine neden olan sürekli açık, hiperaktif yarım kanalların oluşumuna yol açar. Bu durum keratinositlerin proliferasyonu ve farklılaşmasını etkilese de, Cx26 mutasyonlarından kaynaklanan epidermal değişikliklerin altında yatan mekanizmalar henüz bilinmemektedir. Proteomik çalışmalar, Cx26-D50Y KID sendromu mutasyonu içeren HaCaT keratinosit hücre hattında NF-κB sinyal yolağı proteinlerinde zenginleşme olduğunu göstermiştir. Bu nedenle, Cx26 mutant kanallarının NF-κB yolağı aracılığıyla keratinosit proliferasyon ve farklılaşma mekanizmalarını etkileyerek epidermal bozukluklara yol açabileceği hipotez edildi.

Hastalarda farklı şiddetlere neden olan Cx26-G45E and Cx26-D50Y mutasyonlarını sürekli olarak ifade eden HaCaT hücrelerinin proliferasyon ve farklılaşma mekanizmaları üzerinde NF-κB sinyal yolağının rolünü araştırdık. G45E ve D50Y hücreleri sırasıyla çekirdekte bulunan en yüksek RelA ve c-Rel sinyallerini gösterdi. Ek olarak, NaSal muamelesi D50Y hücrelerinde erken ve geç apoptoz oranlarını farklı şekilde etkiledi. Dahası, erken ve geç apoptoz oranları karşılaştırıldığında G45E ve D50Y hücreleri ters yönde bir trend gösterdi. Ayrıca, NF-κB inhibisyonu, G45E hücrelerinin proliferasyon oranını azalttı. Son olarak, NaSal muamelesinden sonra G45E hücrelerinde cytokeratin10 protein seviyelerinde farklılıklar görüldü.

G45E ve D50Y'de NF-κB, apoptozu farklı mekanizmalarla etkileyebilir ve D50Y'nin apoptoz mekanizmaları üzerinde farklı etkiler gösteriyor olabilir. Ayrıca, NF-κB, G45E'nin proliferasyon ve farklılaşma mekanizmalarını düzenliyor olabilir. KID sendromu için mevcut bir tedavi bulunmamaktadır. Bu nedenle, bu çalışma KID sendromunun moleküler ve hücresel mekanizmalarını anlamak açısından önemlidir.

TABLE OF CONTENTS

LIST OF FIGURES

Figure **Page**

Figure **Page**

LIST OF TABLES

Table **Page**

CHAPTER 1

INTRODUCTION

1.1 The Skin

The skin is an effective barrier, protecting our bodies from environmental threats such as dehydration, chemical or physical stress, and pathogens. Additionally, it is important for regulating body temperature and perception of external stimuli (Boulais & Misery, 2008; Sotiropoulou & Blanpain, 2012; Anderton & Alqudah, 2022). The skin consists of three layers, from outer to inner, i.e., the epidermis, the dermis, and the hypodermis (Figure 1.1). All the layers have unique compositions and functions. The dermis and hypodermis form the connective tissue while the epidermis functions as the primary physical barrier that mainly contains keratinocytes (García-Vega et al., 2021; Czyz et al., 2023). These keratinocytes form a stratified epithelium comprising of four layers based on their differential stages: stratum corneum (the outermost layer), stratum granulosum, stratum spinosum, and stratum basale (the deepest layer) (Figure 1.1) (Yousef et al., 2022; Czyz et al., 2023). Stratum corneum is composed of fully differentiated dead keratinocytes with no nuclei. This layer acts as a semipermeable barrier that prevents the entry of external agents and excessive water loss from the body (Menon et al., 2012; Barbieri et al., 2014; Abdo et al., 2020). Stratum granulosum consists of keratinocytes that have more irregular shapes compared to those in stratum spinosum and help creating a permeability barrier via lipid production to prevent water loss. Stratum spinosum contributes to the skin's flexibility and plays role in immune responses. Stratum basale is the location where most mitotic activity in the epidermis occurs and consists of newly formed keratinocytes (Barbieri et al., 2014). Overall, the skin provides four distinct types of barriers which are physical, redox, biochemical (innate immunity), and adaptive immune. The cells forming physical barrier of epidermis is mainly located in the basal and granular layer and are bound together by strong adhesive interactions, facilitated by tight, adherence, and desmosomes (García-Vega et al., 2021). The biochemical, or antimicrobial, layer is composed of lipids, acids,

lysozymes, and antimicrobial peptides. The physical and biochemical barriers together shield against external threats and also prevent the loss of water and solutes (García-Vega et al., 2021; Lee & Kim, 2022).

1.1.1 Epidermal Differentiation

The basal layer of epidermis is separated from the dermis by the basement membrane (basal lamina) and contains mitotically active stem cells which are perpetually producing keratinocytes as mentioned above (Mese et al., 2011; Yousef et al., 2022). Proliferating keratinocytes undergo a differentiation process. Periodically, these cells stop their division and withdraw from the cell cycle, commit to terminal differentiation, migrate outward, and are ultimately shed from the surface of the skin and become specialized cells called corneocytes (Fuchs, 2008; Martin et al., 2014; Faniku et al., 2015; Yasarbas et al., 2024). Differentiated cells which are reaching the skin surface lost their nuclei and packed with keratin filaments (Fuchs, 2008). In this way, epidermis can generate a self-perpetuating barrier that prevent entry of foreign agents and loss of essential body fluids (Fuchs,2008; Abhishek & Palamadai Krishnan, 2016).

During epidermal differentiation, keratinocytes undergo many important morphological and biochemical modifications that involves simultaneous activation and inactivation of numerous proteins and genes (Abhishek & Palamadai Krishnan, 2016; Rousselle et al., 2017). These modifications must occur at the correct time and location to obtain a normal epidermal surface (Rousselle et al., 2017). As a result of the alterations, specific cellular organelles appear which are used as differentiation markers. The members of keratin family, the histidine-rich proteins, the transglutaminases, the cornified envelope precursors (e.g., involucrin, loricrin), and small proline-rich proteins are the most frequently used markers for epidermal differentiation (Lee et al., 1999; Seishima et al., 1999; Rousselle et al., 2017). The expression of the keratin family members is tightly regulated. Cytokeratins 5 and 14 (K5 and K14) are mainly expressed by basal proliferative keratinocytes. When they start to differentiate, keratinocytes switch off cytokeratin K5 and K14 and start expression of cytokeratins 1 and 10 (K1 and K10) in suprabasal layers (Figure 1.1) (Rousselle et al., 2017). Cytokeratins 2, 11, and 9 (K2, K11, and K9) are found in cornified epidermis. Additionally, involucrin and

loricrin are expressed in suprabasal layers and act as envelope precursor proteins (Rousselle et al., 2017). Involucrin is the major cornified envelope precursor protein, and it has been observed that promoter activity of involucrin-encoding gene increased when calcium concentration was raised (Ng et al., 2000). Since involucrin is expressed in nonkeratinized corneal epithelium, it is categorized as an intermediate differentiation marker (Rousselle et al., 2017).

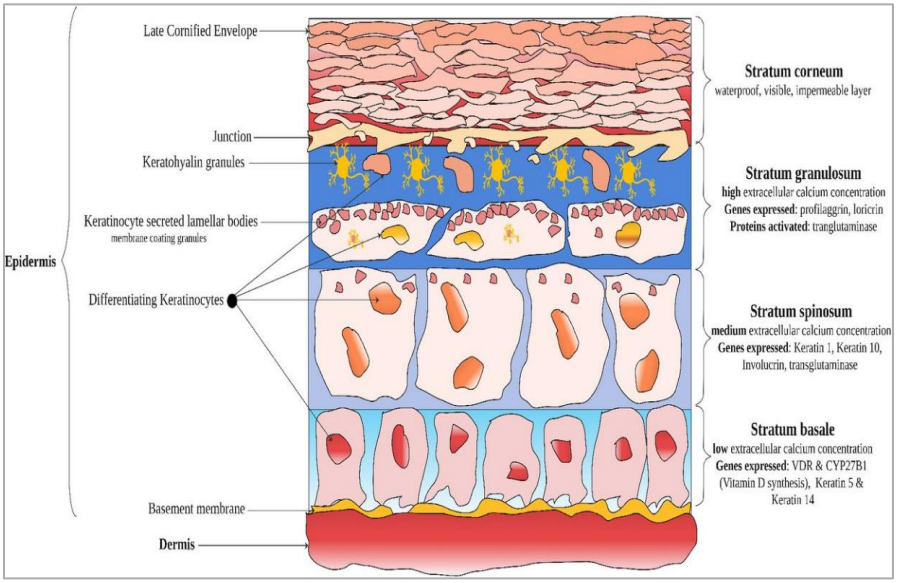

Figure 1.1 The epidermis and dermis form the skin and are separated by a basement membrane. The epidermis consists of four layers: corneum, granulosum, spinosum, and basal. During epidermal differentiation, keratinocytes undergo morphological and biochemical changes that involves simultaneous activation and inactivation of numerous proteins and genes as indicated (Pease et al., 2022).

Mutations in K5 and K14 are linked to a subset of epidermolysis bullosa (EB) which is a skin disease characterized by the separation of the epidermis from the dermis and blistering. Similarly, mutations in K1 and K10 are indicative of epidermolytic ichthyosis, a skin disease that initially characterized with redness and blistering, followed by the progression to hyperkeratosis (Lopez-Pajares et al., 2013). Furthermore, dominant mutations in K10 have been found in ichthyosis with confetti, a rare disease that causes skin redness, blistering, and thickening (Choate et al., 2010). These findings demonstrate that the regulation of genes expressed during epidermal differentiation is essential for maintaining a healthy skin.

1.2 Connexins and the skin

Connexins (Cx) are a family of 21 integral membrane proteins that have an intracellular loop (IL), an amino (N), and a carboxyl (C) termini with four helical transmembrane domains (TM1-TM4) and two extracellular loops (EL1 and EL2) (Figure 1.2.A) (Martin & van Steensel, 2015; Yasarbas et al., 2024). Connexins are synthesized and oligomerize to form structures called connexons, or hemichannels, which possess six connexin subunits in the endoplasmic reticulum (ER)-Golgi network (Martin & van Steensel, 2015; Laird & Lampe, 2022). Each connexins can form homomeric hemichannels by themselves, but also cells can co-express different connexin isoforms which can generate heteromeric connexons, giving diversity to their structure and function (Figure 1.2.B) (Nielsen et al., 2012; Yasarbas et al., 2024). After the formation and trafficking to the plasma membrane, connexons can dock head-to-head with other connexons of adjacent cells and form gap junctions (GJ) (Figure 1.2.C). Hemichannels can be also found in nonjunctional areas and function independently to mediate molecular exchange across the plasma membrane (Donahue et al., 2018; Yasarbas et al., 2024).

GJs are connections that allows the direct transfer of ions, small metabolites, secondary messengers, and short interfering RNAs between neighbouring cells, thus facilitating gap junctional intercellular communication (GJIC) which is essential for various physiological processes such as cell proliferation, differentiation, and cellular homeostasis (Mese et al., 2008; Aypek et al., 2016; García-Vega et al., 2021). Similar to connexons, gap junctions are classified as homotypic or heterotypic depending on the connexon composition (Figure 1.1.C) (Donahue et al., 2018; Laird & Lampe, 2018). Both gap junctions and individual hemichannels are gated. Their opening is dependent on incoming stimuli, including voltage, pH, extracellular calcium, and post-translational modifications (PTMs). Furthermore, each Cx hemichannel subunit shows selective permeability to distinct substances with a maximum molecular weight of 1 kDa (Weber et al., 2004; Loiselle et al., 2013; Donahue et al., 2018). For instance, homotypic Cx32 gap junctions permeate IP_3 much efficiently compared to Cx26 and Cx43 gap junctions in transfected HeLa cells (Niessen et al., 2000). Another study demonstrated that Cx45 and Cx26 are more cation selective, while Cx32 is more anion selective. Cx45 and Cx26 coupled HeLa transfectants showed decreasing permeability to anionic dye

Lucifer Yellow (LY) whereas Cx32 coupled *Xenopus* oocytes showed greater permeability to LY than those coupled by Cx26, suggesting that charge contributes to the selectivity (Cao et al., 1998; Weber et al., 2004).

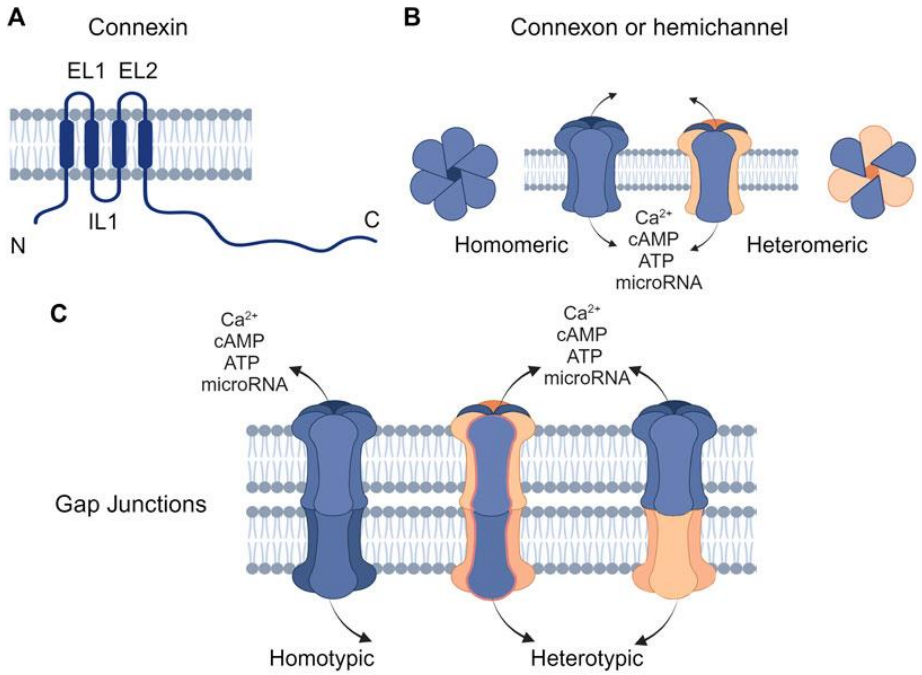

Figure 1.2 Structure of connexins, hemichannels, and gap junctions. (A) Connexins possess an intracellular loop (IL), an amino (N), and a carboxyl (C) termini with four helical transmembrane domains (TM1-TM4) and two extracellular loops (EL1 and EL2). (B) Connexins can hexamerize and form connexons, or hemichannels, which may be either homomeric (consisting of a single type of connexin) or heterotypic (consisting of distinct types of connexins). (C) Connexons on the plasma membrane can dock head-to-head with other connexons of adjacent cells and form homotypic or heterotypic GJ channels (Yasarbas et al., 2024).

The expression patterns of connexins in the epidermis vary notably across its different layers which is crucial for maintaining epidermal homeostasis and facilitating skin renewal (Fuchs, 2008). At least ten different connexins are expressed in the distinct layers of the epidermis during the process of epidermal differentiation. Cx43 is the major connexin expressed in the basal layer, while Cx26, Cx30, Cx30.3, Cx31, Cx31.1, Cx40, Cx43, and Cx45 are primarily expressed in the spinous layer. Transitioning toward granular layer, Cx30.3, Cx31, and Cx43 are highly expressed. In contrary, Cx26, Cx31.1, Cx40, and Cx45 are present at lower levels (Figure 1.3) (Martin et al., 2014; Zhang & Cui, 2017).

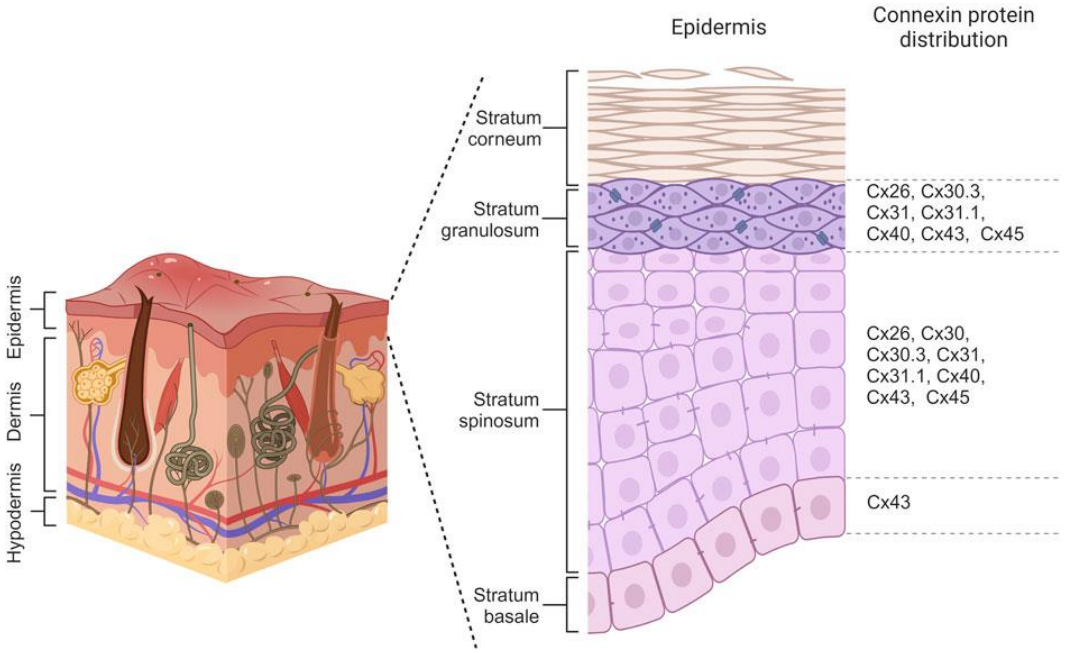

Figure 1.3 Connexin expression patterns within distinct layers of the epidermis. Cx43 is the primary connexin expressed by basal keratinocytes, while Cx26, Cx30, Cx30.3, Cx31, Cx31.1, Cx40, Cx43, and Cx45 are observed in spinosum layer. Cells of granulosum show differential expression of Cx26, Cx30.3, Cx31, Cx31.1, Cx40, Cx43, and Cx45 (Yasarbas et al., 2024).

The functional importance of the various connexin isoforms which are expressed in the epidermis is still under investigation (Yasarbas et al., 2024). The epidermis is consisting of four layers of keratinocytes which are found at different stages of differentiation and have different connexin expression patterns as mentioned previously (García-Vega et al., 2021; Laird & Lampe, 2022). Studies revealed that connexin expressions are dysregulated in various skin conditions such as psoriasis, pressure ulcers and wound healing (García-Vega et al., 2021; Yasarbas et al., 2024). Psoriasis is an inflammatory skin disease characterized by thick, scally lesions. Cx26 showed a dramatic upregulation in psoriatic lesions (Rivas et al., 1997; Labarthe et al., 1998; Lucke et al., 1999; García-Vega et al., 2021). Moreover, mice model overexpressing Cx26 in keratinocytes displayed psoriasis-like phenotypes, further supporting the relation between Cx26 and disrupted barrier function (Djalilian et al., 2006). Connexins are also involved in the complex processes of wound healing (Yasarbas et al., 2024). The expression levels of Cx43 and Cx31.1 decreased at and around the wound site after wounding of the rat tail epidermis. Conversely, Cx26 was upregulated in the

differentiated cells near the wound after injury, while it was downregulated in the cells at the wound edge. *In vivo* dye transfer experiments confirmed that GJIC patterns were also changed compatible with alterations in connexin expression, suggesting that GJIC plays a crucial role in the regulation of epidermal wound healing (Goliger & Paul, 1995). Alterations in connexin activity and compatibility may also cause problems during keratinocyte proliferation (Martin et al., 2014; Chanson et al., 2018; García-Vega et al., 2021). For example, keratinocytes expressing Cx26-R143W, a recessive mutation of *GJB2* that do not cause dermatological signs normally, dramatically increase epidermal thickness in an organotypic co-culture skin model, suggesting enhanced cell proliferation and a delay in terminal differentiation (Man et al., 2007). Another study showed that cellular viability increased in HeLa cells overexpressing Cx26-R143W compared to those overexpressing wild-type Cx26 (Common, 2004). These findings were further supported by another study reporting that induction of Cx26 in repairing human airway epithelial cell (HAEC) cultures was associated with cell proliferation and acts as a negative regulator of HAEC proliferation, suggesting that Cx26 is a fundamental regulator of cell proliferation (Crespin et al., 2014). In a fibroblast wound-healing model, knocking down of Cx43 led to significantly faster healing by enhancing cell migration and proliferation (Mori et al., 2006). Furthermore, studies are showing that connexins can also affect epidermal biology by non-GJ mechanisms through connexin interacting partners. For instance, Cx43, predominantly expressed in most layers, regulates the proliferation and differentiation of keratinocytes by interacting with junctional proteins such as zona occludens, a constituent of tight junctions, and catenins, components of adherens junctions (Hervé et al., 2007; Scott et al., 2012).

These studies revealed that the differential expression of connexins in the skin plays a crucial role in skin physiology and the maintenance of epidermal homeostasis. In addition to their specific distribution and different expression patterns in the skin, connexin gene mutations are also associated with skin-linked diseases, as will be discussed in the next section (García-Vega et al., 2021).

1.3 Connexin mutations in skin diseases

At least ten different connexin isoforms are expressed in humans (Mese et al., 2011; García-Vega et al., 2021), and at least five of them, including Cx26, Cx31,

Cx30.3, Cx43, and Cx30, have been connected to various human epidermal diseases (Avshalumova et al., 2014; Laird & Lampe, 2022; Yasarbas et al., 2024). The epidermis does not have blood vessels and therefore depends on GJIC between keratinocytes to coordinate signals and molecule transfer, for maintaining epidermal homeostasis (Chanson et al., 2018; Qiu et al., 2022). Mutations in associated genes can interfere with GJIC in different ways, resulting in diverse phenotypes. They can cause formation of aberrant hemichannels that allow uncontrolled molecule transfer between inside and outside of the cell. Mutations can also lead to loss of function in protein, thus preventing formation of functional GJs. Furthermore, mutations can cause mislocalization of connexin proteins within the cell and prevent them to reach the cell membrane. As a result, they cannot form GJs. Lastly, mutations can have a dominant-negative effect on the GJIC enhanced by other connexin proteins (Scott et al., 2012; Yasarbas et al., 2024). These alterations disrupt cellular homeostasis and are the reason of pathologies seen in patients.

1.3.1 Connexin26 gene mutations and skin diseases

Cx43 is the most prevalent connexin in human skin; however, mutations and dysregulation in the Cx26, which is normally expressed at very low levels in healthy human epidermis, are linked to several rare syndromic deafness disorders that present with skin pathologies, including abnormal keratinisation and hyperproliferation of the stratum corneum (García-Vega et al., 2021). These involve palmoplantar keratoderma (PPK) with deafness, Vohwinkel's syndrome (VS), Bart-Pumphrey syndrome (BPS), keratitis-ichthyosis-deafness (KID) syndrome, and hystrixlike-ichthyosis-deafness (HID) syndrome, which are classified as gain-of-function diseases in syndromic deafness cases since they cause new features in Cx26-made hemichannels disrupting epidermal homeostasis (Avshalumova et al., 2014; Martin & van Steensel, 2015; Srinivas et al., 2018; Posukh et al., 2023). To date, at least 14 autosomal dominant mutations have been reported in Cx26 that affect the proliferation and differentiation mechanisms of keratinocytes (Yasarbas et al., 2024). Most mutations affect amino acids found on the N-terminus or the first extracellular loop of the polypeptide. These residues have role in assembly of connexons, transport of connexins to the plasma membrane, connexon-connexon interactions between adjacent cells, voltage gating, and

regulating the opening of hemichannel pores which is important to control channel permeability (Richard et al., 2004; Thomas et al., 2004; Lee & White, 2009; Avshalumova et al., 2014; Dalamón et al., 2016, Srinivas et al., 2018; Yasarbas et al., 2024). Palmoplantar keratoderma (thickened skin on the palms and soles) and autosomal dominant sensorineural hearing loss are typical features of syndromic deafness disorders linked to Cx26 gene mutations and associated skin diseases. Additional skin phenotypes can be observed depending on the mutation and the related disease (Richard et al., 2004; Scott et al., 2012; Avshalumova et al., 2014; Srinivas et al., 2018; Cammarata-Scalisi et al., 2020).

1.4 Keratitis-Ichthyosis-Deafness (KID) Syndrome

Keratitis-ichthyosis-deafness (KID) syndrome is a rare genetic disorder characterized by vision problems, abnormal skin phenotype, and sensorineural deafness (García et al., 2016). The first case of KID syndrome was reported in 1915. The report was about a 16-years old boy who suffered from congenital keratoderma beside severe deafness and keratitis (Burns, 1915; Caceres-Rios et al., 1996). Keratitis is defined as a corneal inflammation causing severe pain, light sensitivity, scarring, neovascularization, and conjunctivitis. Some patients may lose their sight completely depending on the severity of the disease (García et al., 2016; Srinivas et al., 2018). The most common skin phenotypes are palmoplantar keratoderma (PPK), thickening of palms and soles, with thickened dry (ichthyosis) reddish patches on the skin (erythrokeratoderma). Scarring alopecia (hair loss) may also be observed due to hyperkeratosis on follicles and recurring bacterial, viral, or fungal infections (Caceres-Rios et al., 1996; Avshalumova et al., 2014; Srinivas et al., 2018). KID syndrome patients have high tendency to develop squamous cell carcinoma (SCC), and this symptom differs KID syndrome from other skin disorders with similar skin phenotypes called as the erythrokeratodermas (Van Geel et al., 2002; Nyquist et al., 2007; Avshalumova et al., 2014).

KID syndrome is inherited in an autosomal dominant manner and is caused by mutations in *GJB2* encoding Cx26 protein (Mazereeuw-Hautier et al., 2007; Yasarbas et al., 2024). The severity of the disease varies significantly among individuals with KID syndrome (Lilly et al., 2016). Cx26-G45E is one of the most severe mutations causing the formation of hyperactive hemichannels and GJ channels due to high cell membrane

current (Stong et al., 2006). The increased membrane current and constantly open hemichannels disrupted cellular homeostasis, and eventually led to cell lysis and death. Noticeably, increase in extracellular Ca^{+2} levels could moderate the severe symptoms by promoting the closure of hyperactive hemichannels (Stong et al., 2006; Gerido et al., 2007; Jonard et al., 2008; Mese et al., 2011; Sanchez & Verselis, 2014; Taki et al., 2018). A transgenic mouse model expressing Cx26-G45E have been generated. The mutation reduced viability specifically in keratinocytes and resulted in hyperkeratosis, skin scaling, and scarring alopecia, thereby resembling the pathological characteristics of KID syndrome. In addition, hemichannel activity was increased in the transgenic keratinocytes, further proving the role of raised hemichannel activity in the pathogenicity of the Cx26-G45E mutation (Mese et al., 2011). Similar to Cx26-G45E, the Cx26-A88V mutation resulted in hyperactive cell membrane due to formation of aberrant hemichannels. Both mutations can manifest severe phenotypes, including severe skin infections which can progress into septicaemia, and eventually death in the affected individuals (Jonard et al., 2008; Mese et al., 2011; Mhaske et al., 2013; Lilly et al., 2019; Cammarata-Scalisi et al., 2020). On the other hand, patients with Cx26-D50Y and Cx26-I30N revealeed milder symptoms (Yotsumoto et al., 2003; Arndt et al., 2010; Aypek et al., 2016). Dye uptake assays showed that Cx26-D50Y and Cx26-I30N mutations increased dye uptake compared to wild type cells, suggesting abnormal hemichannel activities similar to those in the Cx26-G45E and Cx26-A88V mutations. Immunostaining experiments also showed that Cx26-D50Y and Cx26-I30N failed to form gap junction plaques at cell-cell junctions. Moreover, these mutations prevented the trafficking of Cx26 and caused the protein to be retained in the Golgi apparatus (Aypek et al., 2016). Cx26-S17F is another type of Cx26-KID syndrome mutation manifesting milder phenotypes in affected individuals (Lilly et al., 2016). In a mouse model carrying the Cx26-S17F mutation, heterozygous animals displayed epidermal hyperplasia on their tails and footpads. Adult mice also developed hearing disablement, potentially due to disrupted ionic homeostasis in the inner ear (Schütz et al., 2011). Another mouse model which expresses Cx26-S17F under the control of cytokeratin14 promoter displayed abnormal keratinocyte proliferation and differentiation in footpads of animal (Press et al., 2017). Furthermore, Cx26 had wider distribution compared to control animals. In contrast with other KID syndrome mutations that cause hyperactive hemichannels, the Cx26-S17F mutation impaired intercellular coupling although the proper intracellular transport of the protein within the cell (Richard et al., 2002; Schütz

et al., 2011; García et al., 2015). Surprisingly, when Cx26-S17F is co-expressed with wild-type Cx26 or Cx43, hyperactive hemichannel formation was observed (García et al., 2015).

Functional studies on Cx26-KID syndrome mutations revealed that these mutations lead to formation of “leaky” hemichannels on the cell membrane which promote uncontrolled molecule transfer between the inside and the extracellular environment of the cell. As a result, cellular homeostasis is disrupted and cell death occurs, but also the behaviour of surrounding cells is affected, interrupting the proliferation and differentiation of keratinocytes (Yasarbas et al., 2024). However, the underlying mechanisms that cause epidermal changes in KID syndrome due to Cx26 mutations are not fully known.

1.5 NF-κB signaling pathway

Nuclear Factor kappa B (NF-κB) was first described as a factor in the nucleus of B cells which binds to the enhancer region of the kappa light chain of immunoglobulin (Sen & Baltimore, 1986). NF-κB family is a group of transcription factors that are found in the cytoplasm of nearly all cell types. It is evolutionarily conserved in all animals from fruit fly to humans (Espín-Palazón & Traver, 2016). Since the discovery of NF-κB family, it has been found to have significant roles in various physiological and pathological processes such as development, regulation of immune responses and inflammation, cell survival, proliferation, and differentiation (Oeckinghaus & Ghosh, 2009; Ben-Neriah & Karin, 2011; Hayden & Ghosh, 2011; Guo et al., 2024). Bacterial and viral infections, inflammatory cytokines, and antigen-receptor engagement can activate NF-κB pathway, proving its importance for innate and adaptive immune responses. This pathway can also be activated upon physical (e.g., UV light), physiological (e.g., ischemia), or oxidative stress (Robert & Kupper, 1999; Hayden et al., 2006; Oeckinghaus & Ghosh, 2009; Espín-Palazón & Traver, 2016). Consistent with the great number of signals activating the pathway, target genes controlled by NF-κB is also broad. The list of target genes includes regulators of apoptosis (Bcl family members) and proliferation (cyclins and growth factors), confirming the role of NF-κB in cell growth, proliferation, and survival of the cell (Espín-Palazón & Traver, 2016). Therefore, it is comprehensible that dysregulation in NF-κB pathway causes serious

diseases, including arthritis, immunodeficiency, autoimmunity, and cancer (Courtois & Gilmore, 2006). Due to its capacity to affect the expression of numerous genes, NF-κB activity is tightly regulated at various levels. The primary regulatory mechanism is through inhibitory IκB (inhibitor of NF-κB) proteins and the I-kappaB kinase (IKK) complex, which consists of IKKα, IKKβ, and NEMO (IKKγ) (Figure 1.4.A) (Oeckinghaus & Ghosh, 2009; Shen et al., 2023; Guo et al., 2024). Post-translational modifications also regulate the IκB and IKK activities, as well as the NF-κB members themselves (Oeckinghaus & Ghosh, 2009).

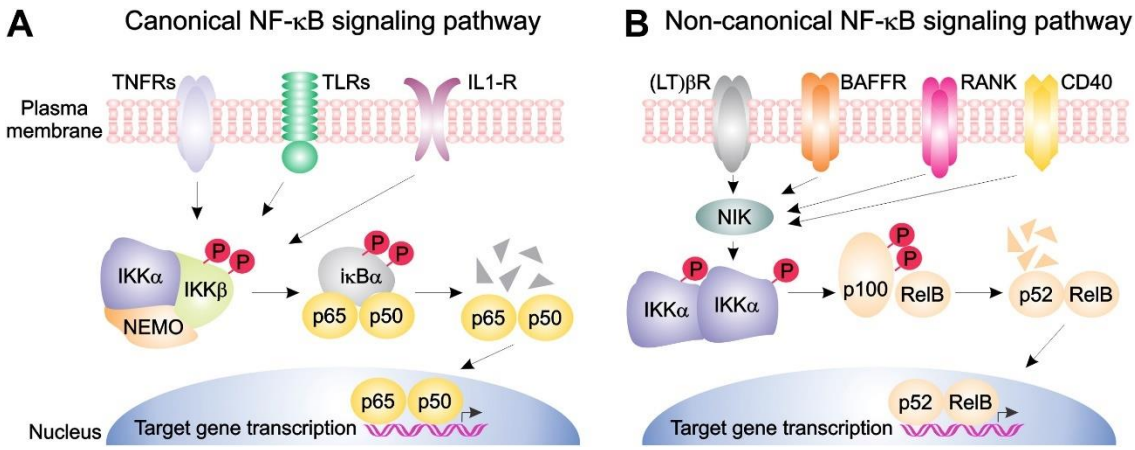

Figure 1.4 Canonical versus non-canonical NF-κB signaling. (A) The activation of canonical NF-κB receptors, such as TNFRs, TLRs, or IL1-R, by their specific ligands leads to the activation of IKKβ. Activated IKKβ then phosphorylates IκBα resulting in its separation from p65/p50 complex and degradation. After releasing, p65/p50 heterodimers can translocate to the nucleus and exert their function on the target gene. (B) The activation of noncanonical NF-κB receptors (LT)βR, BAFFR, RANK, CD40 activate NIK and triggers phosphorylation of IKKα. Activated IKKα phosphorylates p100, causing its polyubiquitination and subsequent processing to generate p52. Heterodimers of p52/RelB translocate to the nucleus to regulate their target gene expression (Espín-Palazón & Traver, 2016).

NF-κB pathway in mammals consists of five Rel protein family members: p50 (active form of p105), p52 (active form of p100), RelA (p65), RelB, and c-Rel. These factors can function as homodimers or heterodimers and are found inactive in the cytoplasm. Once the pathway is activated and they translocate to the nucleus, they induce or repress expression of their specific target gene by binding to the classical κB sites or to noncanonical sequences (Pahl, 1999; Wong et al., 2011; Guo et al., 2024). All

members carry a common feature which is a conserved sequence (~300 amino acids) at the N-terminal called as Rel homology domain (RHD). This sequence is important for the binding of NF-κB members to other proteins and target DNA (Wang et al., 2019). NF-κB is activated in cells through two distinct mechanisms, canonical and non-canonical (Figure 1.4) (Shen et al., 2023). These pathways differ in their receptors triggered by the upcoming signal, the downstream intermediate elements, and the NF-κB family members they subsequently activate (Brown et al., 2008). In the canonical pathway, the heterodimers of p50 and p65 are kept inactive in the cytoplasm through their interaction with IκBα (Figure 1.4.A). When the signal reaches the cell membrane, IKKβ (inhibitor of NF-κB kinase subunit beta) is activated by a downstream effector of canonical NF-κB receptors such as TLRs, antigen receptors, cytokine receptors, or growth factor receptors. Activated IKKβ then phosphorylate IκBα and cause release of IκBα from the p50/p65 complex (Figure 1.4.A). Thus, p50/p65 complex translocates to the nucleus and exert their functions on the target genes (Figure 1.4.A). Similarly, in the non-canonical pathway, p100/RelB complex is retained inactive in the cytoplasm until p100 is phosphorylated and partially processed into the active p52/RelB form, which then translocates to the nucleus to exert its function as a transcription factor (Figure 1.4.B). The difference is that phosphorylation of p100/RelB complex is dependent on NF-κB-inducing kinase (NIK) and IKKα (NF-κB kinase subunit alpha) (Figure 1.4.B) (Espín-Palazón & Traver, 2016; Guo et al., 2024).

Several studies have shown that inhibition of NF-κB pathway in non-immune, epithelial or parenchymal cells promote development of severe inflammatory conditions spontaneously. These findings are showing the versatile roles of NF-κB signaling, and they indicate that NF-κB inhibition in specific tissues may exert proinflammatory effects by disrupting physiological immune homeostasis in the cell (Oeckinghaus & Ghosh, 2009).

1.5.1 The role of NF-κB signaling pathway in skin physiology

The skin acts as an effective barrier that shields against a wide range of chemical, microbial, and physical threats. It can be regarded as a major component of the innate host defence system and serves as a major physical mediator to initiate stress-

associated signals (Bell et al., 2003). The skin must hold a balance between cell proliferation and cell loss due to desquamation, shedding or peeling off of the stratum corneum, while responding to the environmental stimuli (Seitz et al., 1998). In stratified epithelium, proliferative basal keratinocytes enter cell cycle arrest as they migrate outward and activate genes responsible for terminal differentiation as mentioned previously. Abnormalities in these processes disrupt epidermal homeostasis and may result in various inflammatory skin diseases (Seitz et al., 1998; Bell et al., 2003). Expression of NF-κB is not limited to the immune system. Various non-haemopoietic tissues, including skin and other ectoderm-derived tissues, also depend on NF-κB for maintaining cellular homeostasis (Wright et al., 2019; Shen et al., 2023). Several studies have revealed that members of NF-κB family have significant roles in regulating epidermopoiesis which is the process of formation and development of epidermis involving the proliferation, differentiation, and maturation of keratinocytes (Bell et al., 2003; Gugasyan et al., 2004). In an A20-deficient mouse model, which fail to terminate TNF-induced NF-κB activity, a sustained NF-κB activity, thickened epidermis and dermis, and loss of hair follicles have been observed (Lee et al., 2000). In normal murine skin, p50 was found to be located in the cytoplasm of basal keratinocytes, while cytoplasmic expression was absent in differentiating and mitotically inactive suprabasal keratinocytes. Additionally, nuclear expression of NF-κB has been demonstrated in these cells (Seitz et al., 1998). In a transgenic mice model, which express IκBα mutant resistant to degradation, epidermal hyperplasia developed shortly after birth. These animals had thickened suprabasal squamous layer, and they were deficient in normal hair formation. Consistent with these results, inhibition of NF-κB in normal adult murine skin and in grafted human epidermal cells resulted in hyperplastic epithelium. On the other hand, transgenic mice, which overexpress active p50 or p65 in the nucleus of skin cells, developed epidermal hypoplasia and died prematurely. Their epidermal cells had almost no DNA synthesis, suggesting an inhibition of cellular proliferation (Seitz et al., 1998). These findings suggested that nuclear NF-κB may be required for the growth inhibition control during outward migration and differentiation of keratinocytes (Bell et al., 2003). IKKα lacking mice developed a thickened stratum spinosum and could not form the granular and corneal layers (Hu et al., 1999; Li et al., 1999; Gugasyan et al., 2004). Another study further showed that IKKα-deficient mice exhibited increased proliferation in epidermal keratinocytes but prevented their terminal differentiation (Hu et al., 2001). IKKγ-deficient (*ikkγ*$^{+/-}$) female mice similarly

exhibited skin defects, including epidermal hyperproliferation, hyperkeratosis, hyperpigmentation, and inflammation, alongside increased apoptosis rates in keratinocytes (Schmidt-Supprian et al., 2000). Mice lacking p65 and c-Rel had mutant basal keratinocytes that were abnormally small, showed a delay in G1 progression, and could not form colonies in culture, suggesting that c-Rel and RelA are important for skin development and homeostasis (Gugasyan et al., 2004). Also, CRE-mediated deletion of p65 and c-Rel under the control of K14 promoter in keratinocytes of mutant mice resulted in severe dermatitis with some characteristics of psoriasiform, further highlighting the significant role of canonical NF-κB members in the maintenance of skin homeostasis (Grinberg-Bleyer et al., 2015). Moreover, downregulation of c-Rel leads to increased apoptosis rates, a delay in the G2/M phase of the cell cycle with reduced proliferation, and abnormal mitotic spindle formation in HaCaT keratinocytes (Lorenz et al., 2015). RelB-deficient mice (*relB*$^{-/-}$) had skin inflammation (Weih et al., 1997). Also, thickened skin and hair loss have been observed. Immunohistochemical analysis of skin lesions displayed hyperkeratosis and marked epidermal hyperplasia (Barton et al., 2000).

Overall, these studies revealed that NF-κB pathway is important for the proliferation and differentiation of the mammalian skin, and a balanced NF-κB activity is required for skin homeostasis (Bell et al., 2003; Sur et al., 2008).

1.6 Aim of the study

KID syndrome is a rare genetic disease characterized by several symptoms, including abnormal thickening of the epidermis, known as hyperkeratosis. The disease arises from Cx26 mutations causing formation of "leaky" hemichannels on the cell membrane, allowing uncontrolled molecule transfer between the inside and outside of the cell (Yasarbas et al., 2024). This uncontrolled molecule transfer disrupts epidermal homeostasis by affecting the proliferation and differentiation of keratinocytes, but the exact molecular and cellular mechanisms underlying the epidermal alterations observed in Cx26 mutations-induced KID syndrome are not known yet. NF-κB pathway has important roles in skin physiology as mentioned above. Proteomic studies have shown enriched NF-κB pathway molecules in keratinocyte cell line HaCaT expressing Cx26-D50Y mutation compared to Cx26-WT cells. Therefore, it is hypothesized that mutant

Cx26 channels may lead to epidermal diseases by altering proliferation and differentiation mechanisms of keratinocytes via NF-κB pathway. Based on the hypothesis, it is aimed to investigate the effects of the NF-κB signaling pathway on the proliferation and differentiation mechanisms of the HaCaT keratinocyte cell lines that constitutively express Cx26-D50Y and Cx26-G45E mutations, which cause different severity in patients.

CHAPTER 2

MATERIALS AND METHODS

2.1 Maintenance of HaCaT Cell Line

Immortalized human keratinocyte cell line, HaCaT cells, were used in this study. HaCaT cells were cultured in high glucose Dulbecco's Modified Eagle Medium (DMEM) (Gibco, 41966029) supplemented with 10% Fetal Bovine Serum (FBS; Serox, SF101H-500), 1% Penicillin/Streptomycin (P/S; Gibco, 15140122), and a low concentration of calcium (3.2 mmol/L) to keep hemichannels close and thus help cell growth. Cells were incubated in a humidified environment with 5% CO_2 at 37 °C. HaCaT cells were infected with MSCV retroviral vector that contain Cx26-WT, Cx26-G45E, and Cx26-D50Y cDNAs. The cells which were infected with MSCV-Cx26-WT correspond to WT, MSCV-Cx26-G45E to G45E, and MSCV-Cx26-D50Y to D50Y in the text. The cells carrying empty MSCV vector was used as a control group and correspond to MSCV.

When HaCaT cells enter their log phase, they were split after 20 minutes incubation with 0.05% EDTA solution (Biological Industries, 03-015-1B) and 3-5 minutes incubation with 0.25% Trypsin-EDTA solution (Gibco, 25200056), respectively, in a humidified environment with 5% CO_2 at 37 °C.

2.2 Immunostaining and Fluorescence Microscopy

HaCaT cells (2 x 10^5 per well) were seeded on coverslips in 6-well plates and cultured for 48 hours. Later on, cells were washed with 1-2 mL of 1X PBS twice and were fixed with 500-600 µl of 4% paraformaldehyde (PFA) for 20 minutes at room temperature. Cells were then washed again with 1 mL of 1X PBS three times, permeabilized with 1 mL of 0.1% Triton X-100/PBS for 15 minutes, and blocked in 3% BSA prepared in 0.1% Triton X-100/PBS for 30 minutes at room temperature, respectively. After that, cells were incubated with primary antibody (Table 2.1) diluted

in 3% BSA overnight at 4 °C. In some experiments, actin filaments were also stained with 1:300 dilution of Alexa Fluor 488 conjugated Phalloidin (Invitrogen, A12379) to make cell boundaries apparent. On the following day, cells were washed with 1 mL of 1X PBS and were incubated with 1:200 dilution of Alexa Fluor 555-conjugated rabbit anti-mouse secondary antibody (Life Technologies, A21427) and 1:1000 dilution of 1 µM 4′,6-Diamidino-2-Phenylindole (DAPI; Sigma, D9542) for 45 minutes at room temperature in dark. Then, cells were washed with 1 mL of 1X PBS three times and mounting was done onto slides after coverslips were dipped into distilled water. Finally, the staining was verified under fluorescence microscope (IX83, Olympus, Japan) with 20x or 100x oil-immersion objectives. The images were taken by a CCD digital camera and were analysed by using ImageJ program.

Table 2.1 List of primary antibodies used in immunostaining experiments.

Antibody	**Concentration**	**Host**	**Class**	**Supplier**
Anti-RelA	1:100	Mouse	polyclonal	Santa Cruz Biotechnology (sc-8008)
Anti-RelB	1:100	Mouse	polyclonal	Santa Cruz Biotechnology (sc-48366)
Anti-c-Rel	1:100	Mouse	polyclonal	Santa Cruz Biotechnology (sc6955)
Anti-cytokeratin10	1:300	Mouse	polyclonal	Abcam (ab9025)
Anti-cytokeratin14	1:300	Mouse	polyclonal	Abcam (ab7800)
Anti-involucrin	1:350	Mouse	polyclonal	Abcam (ab68)

2.3 BrdU Assay

HaCaT cells (2 x 10^5 per well) were seeded on coverslips in 6-well plates and cultured for 48 hours in DMEM without calcium. Later on, the old medium was replaced with the freshly prepared medium containing 10 mM of NaSal, and cells were incubated for 6 hours. After 3 hours incubation with NF-κB inhibitor, BrdU was added to culture medium. Final concentration of BrdU in medium was adjusted to 20 µM. After addition of BrdU, cells were incubated 3 more hours. At the end of incubation, cells were washed with 1 mL of 1X PBS for 3 minutes twice. Then, cells were fixed

with 750 µl of 4% paraformaldehyde (PFA) for 45 minutes at room temperature. After fixation, cells were washed with 1 mL of 1X PBS for 5 minutes three times. Cells were treated with 1 mL of 1.5 M HCl for 30 minutes and were washed with 1 mL of PBS for 5 minutes twice. To block non-specific epitopes, 5% normal horse serum (NHS) containing PBS, 0.1% Triton X-100, and NHS was prepared, and 750 µl of 5% NHS was added into each well. After 1 hour blocking, cells were washed with 1 mL of 1X PBS once. For antibody treatment, 2% NHS containing required amount of anti-BrdU antibody solution (1:50) (APC eBioScience, 15-5071-41) was prepared, and each cover glass was incubated with 150 µl of antibody solution at room temperature overnight.

After overnight incubation, cells were washed with 1 mL of 1X PBS for 5 minutes three times. Then, cells were incubated with 1:600 dilution of Alexa Fluor 555-conjugated goat anti-mouse secondary antibody and 1:1000 dilution of DAPI prepared in 2% NHS for 45 minutes at room temperature in dark. Then, cells were washed with 1 mL of 1X PBS for 5 minutes three times and mounting were done onto slides after coverslips were dipped into distilled water. Finally, the staining was verified under fluorescence microscope (IX83, Olympus, Japan) with 4x objective. The images were taken by a CCD digital camera and were analysed by using ImageJ program.

2.4 MTT Assay

HaCaT cells (2 x 10^3 per well) were seeded into 48-well plate as two replicas and three sets (for day 1, 4 and 7) for each cell type. Cells were cultured in DMEM with required amount of calcium and NF-κB inhibitor 0.5 mM sodium salicylate (NaSal; Sigma-Aldrich, 71945-250G) for 7 days. At day 1, 10% MTT solution was prepared in the required amount of DMEM, and the old medium was replaced with 500 µl of 10% MTT solution. Cells were then incubated for 4 hours in a dark humidified environment with 5% CO_2 at 37 °C. After 4 hours of incubation, MTT solution was removed, and 200 µl dimethyl sulfoxide (DMSO; Serva, 3975701) was added into each well to dissolve tetrazolium salts. Pipetting was done very well and 100 µl of solution was loaded into 96-well plate as 2 replicas from each well. In addition, 100 µl of DMSO was loaded into one well as a blank. Colorimetric measurement was performed at 570 nm and 650 nm by using Thermo ELECTRON CORPORATION Multiskan Spectrum instrument. The data was normalized to day 1 of each sample to make an accurate

comparison between control group and mutation carrying cells.

2.5 PI Staining and Cell Cycle Analysis

HaCaT cells (4 x 10^5 per well) were seeded in 6-well plates and cultured for 48 hours in DMEM without calcium. Later on, the old medium was replaced with the freshly prepared medium containing 10 mM of NaSal, and cells were incubated for 6 hours. After incubation with NF-κB inhibitor, cells were washed and incubated with 0.05% EDTA for 20 minutes. Then, cells were trypsinized and collected into falcon tubes. Centrifugation was done for 10 minutes at 1,200 rpm. Supernatant was removed and pellet was dissolved with 1 mL of ice cold 1X PBS on ice. Later on, 4 mL of ice cold 100% ethanol (EtOH) was added onto cell suspension and mixed for fixation of cells. Samples were stored at -20 °C at least overnight. They can be stored up to 1 week at -20 °C.

After overnight incubation, samples were centrifuged for 10 minutes at 1,500 rpm and then for 1 minute at 2,000 rpm at 4 °C, respectively. Supernatant was removed and pellet was gently dissolved with 1 mL of cold 1X PBS. Then, cell suspension was transferred into Eppendorf tube and centrifuged for 10 minutes at 1,500 rpm at 4°C. Supernatant was discarded, and cell pellet was dissolved with 200 µl 0.1% Triton X-100/PBS. Next, 20 µl 200 µg/mL RNaseA (Macherey-Nagel, 740505) was added, and the cell suspension was incubated for 30 minutes at 37 °C. After 30 minutes, 20 µl of 1 mg/mL propidium iodide (PI; Invitrogen, P1304MP) solution was added and incubated for 15 minutes at room temperature in dark. Finally, cell cycle analysis was performed by using FACS Canto instrument (BD Biosciences, CA, USA).

2.6 Apoptosis Analysis

HaCaT cells (4 x 10^5 per well) were seeded in 6-well plates and cultured for 48 hours in DMEM without calcium. Later on, the old medium was replaced with the freshly prepared medium containing 10 mM of NaSal, and cells were incubated for 6 hours. After incubation with NF-κB inhibitor, cells were washed and incubated with 0.05% EDTA for 20 minutes. Then, cells were trypsinized and collected into falcon

tubes. Centrifugation was done for 5 minutes at 0,3 rcf. Supernatant was removed and pellet was washed twice with 1 mL of cold 1X PBS and centrifuged for 5 min at 1,600 rpm. Then, the cells were stained by following PE Annexin V Apoptosis Detection Kit with 7-AAD protocol (BioLegend, 640934). Finally, apoptosis analysis was performed by using FACS Canto instrument (BD Biosciences, CA, USA).

2.7 Q-RT PCR Analysis

HaCaT cells (4 x 10^5 per well) were seeded in 6-well plates and cultured for 48 hours in DMEM without calcium. Later on, the old medium was replaced with the freshly prepared medium containing 10 mM of NaSal, and cells were incubated for 6 hours. After incubation with NF-κB inhibitor, cells were washed with 1 mL of cold 1X PBS and flash frozen with liquid nitrogen. Samples were stored at -80 °C until nucleic acid isolation.

Total RNA was isolated using Monarch® Total RNA MiniPrep Kit (New England Biolabs, T2010S). Protocol that is provided by the manufacturer was followed. After isolation, RNA concentrations of the samples were measured by Nanodrop instrument. Next, cDNA from 1 µg of RNA samples was synthesized by using RevertAid First Strand cDNA Synthesis Kit (Thermo Scientific, K1622). Quantitative real-time PCR was performed, and cDNA samples were amplified by using RealQ Plus 2x Master Mix Green (Ampliqon, APQ-A323402). Prepared mix was conducted for 40 cycles by Roche Real Time PCR System. TATA-Box Binding Protein (TBP) gene, that is a housekeeping gene, was used as control beside gene of interests. Cycle time (Ct) values of interested gene were normalized to the Ct values of TBP gene. Fold changes were calculated by using the formula below:

$$2^{-\Delta\Delta Ct} = 2^{\text{control group (interested gene Ct value - TBP gene Ct value) - experimental group (target gene Ct value - TBP gene Ct value)}}$$

PCR conditions and used primers are shown in Table 2.2 and Table 2.3, respectively.

Table 2.2 Cycle conditions for Q-RT PCR.

Stage	Temperature	Duration	Cycle
Pre-incubation	95 °C	900 seconds	1 cycle
Three-step amplification	95 °C	30 seconds	45 cycles
	60 °C	30 seconds	
	72 °C	30 seconds	
Melting	95 °C	10 seconds	1 cycle
	65 °C	60 seconds	
	72 °C	1 second	

Table 2.3 Sequences of forward and reverse primers of interested genes used in Q-RT PCR.

Name of Gene	Forward Primer	Reverse Primer
Human TBP	5'-tagaaggccttgtgctcacc-3'	5'-tctgctctgactttagcacct-3'
Involucrin	5'- tctgcctcagccttactgtg-3'	5'- cagtggagttggctgtttca-3'
Cytokeratin10	5'- gccaacatcctgcttcagat-3'	5'- ggctctcaatttgcatctcc-3'
Cytokeratin14	5'- cctctcctcctcccagttct-3'	5'- gatcttccagtgggatctgtgt -3'

2.8 Western Blot Analysis

2.8.1 Protein Isolation

HaCaT cells (6 x 10^5) were seeded into 6-cm dishes containing 5 mL of DMEM without calcium and cultured for 48 hours. Later on, the old medium was replaced with the freshly prepared medium containing 10 mM of NaSal, and cells were incubated for 6 hours. After incubation with NF-κB inhibitor, cells were trypsinized and centrifuged for 2 minutes at 3,000 rpm. Supernatant was removed, and 1 mL of 0.05% EDTA was added into falcons. Centrifugation was performed for 1 minutes at 3,000 rpm, and supernatant was removed again. Pellet was dissolved with 100 µl master mix, that contains 495 µl of lysis buffer (10 mM Tris-HCl, 1 mM EDTA, 0.1% Triton-X), 5 µl of Protease Inhibitor (PI; Sigma, P8340-5ML), and 0.5 µl of DL-Dithiothreitol solution

(DTT; 1.04 g/mL; Sigma, 43816-10ML). Cell suspension was mixed very well and incubated on ice for 20 minutes. Then, samples were centrifuged at 14,000 rpm for 20 minutes. Finally, supernatant was taken and stored at -80 °C for further analysis.

2.8.2 Bradford Assay

In the first part of Bradford assay, BSA (20 mg/mL) (New England Biolabs, B9000S) with different concentrations that are 4 mg/mL, 2 mg/mL, 1 mg/mL, 0.5 mg/mL, 0.25 mg/mL were prepared for a standard curve. Then, 800 µl of autoclaved distilled water, 200 µl of 5X Bradford reagent (Serva, 3922202), and 10 µl of BSA with different concentrations were mixed in glass cuvettes, and the standard curve was created by Thermo Scientific GENESYS 10S VIS Spectrophotometer instrument. After that, 10 µl of protein samples prepared in Bradford solution were measured with the same way. Protein concentrations were measured at 570 nm by using the same instrument.

2.8.3 Western Blotting

12% resolving and 5% stacking SDS gels were prepared. First, samples and 5X loading dye were heated at 95 °C for 5 minutes. Before loading into the gel, protein concentrations of samples were set to one with the lowest concentration (25-40 µg/mL). Then, required amount of 5X loading dye was added into samples, and samples were loaded into the gel. The gel was run at 40 V for 1-1.5 hours, 60 V for 10 minutes, and 90 V for 20-30 minutes, respectively. After running of samples, they were transferred to nitrocellulose membrane (EcoTech Biotechnology, NC045) at 90 V for 2 hours. Then, samples were blocked with 3% BSA dissolved in 1X Tris Buffer Saline-Tween20 (TBS-T) for 1 hour at room temperature. Next, membranes were incubated with 1:1000 dilution of primary antibody against cytokeratin14 (1:1000; Abcam, ab7800) or beta-actin (1:1000; Abcam, ab8227) for 16 hours at 4°C.

After 16 hours of incubation, membranes were washed with 1X TBS-T three times for 10 minutes. Then, membranes were incubated with 1:1000 dilution of anti-mouse (DAKO, P0447) or anti-rabbit secondary antibody (Thermo Scientific, 31460)

for 2 hours at room temperature. Finally, membranes were washed with 1X TBS-T three times for 10 minutes, and membranes were displayed with chemiluminescence (Bio-Rad, 1705061) by using FUSION SL VILBER LOURMAT imaging system.

2.9 Statistical Analysis

In this study, all experiments were performed as triplicates. The results were reported as mean± standard deviation, and the differences between WT and other groups were statistically evaluated by unpaired t-test. “n” refers to the total number of experiments. “p” values refer to the statistical significance of experiments, and they are detailed in each figure legend.

CHAPTER 3

RESULTS

3.1 SECTION I

3.1.1 The role of NF-κB in HaCaT cells overexpressing WT Cx26 and KID Syndrome mutations G45E and D50Y.

Once the NF-κB pathway is activated, NF-κB transcription factors translocate to the nucleus, and they induce or repress expression of their specific target genes (Guo et al., 2024). Therefore, to understand the activity of NF-κB in HaCaT cells expressing WT, G45E, and D50Y constructs, the localization of NF-κB members RelA (p65), RelB, and c-Rel was examined by performing immunostaining with suitable antibodies. Then, the ratio of nuclear fluorescence intensity to total fluorescence intensity was calculated for all cells, and the fold differences were determined by normalizing to MSCV cells. In addition, the cells were stained with Alexa Fluor 488 conjugated Phalloidin to visualize cells' boundaries, and the nuclei of the cells was stained with DAPI. Then, all the images were merged.

RelA protein showed more cytosolic localization in MSCV and D50Y cells, while WT and G45E cells exhibited a diffused pattern between nucleus and cytoplasm (Figure 3.1.1). The fluorescence intensity of nuclear RelA is 16% higher and 8% lower in G45E and D50Y, respectively, compared to WT. Among all the cells, G45E had the highest nuclear/total fluorescence intensity ratio. Additionally, MSCV showed significantly lower nuclear RelA signal compared to WT (Figure 3.1.1). RelB protein exhibited a diffused pattern in MSCV and G45E. On the contrary, WT and D50Y revealed more nuclear localization (Figure 3.1.2). The fluorescence intensity of nuclear RelB is 13% and 5% higher in WT compared to G45E and D50Y cells, respectively. In addition, all the cells had a higher nuclear/total fluorescence intensity ratio compared to MSCV. Moreover, WT had significantly higher nuclear RelB signal compared to MSCV (Figure 3.1.2). Finally, c-Rel protein showed more nuclear localization pattern in

MSCV, G45E, and D50Y (most prominent one), while WT exhibited a diffused pattern compared to the others (Figure 3.1.3). The fluorescence intensity of nuclear c-Rel is the lowest in WT. The ratio was 8% and 28% higher in G45E and D50Y, respectively (Figure 3.1.3).

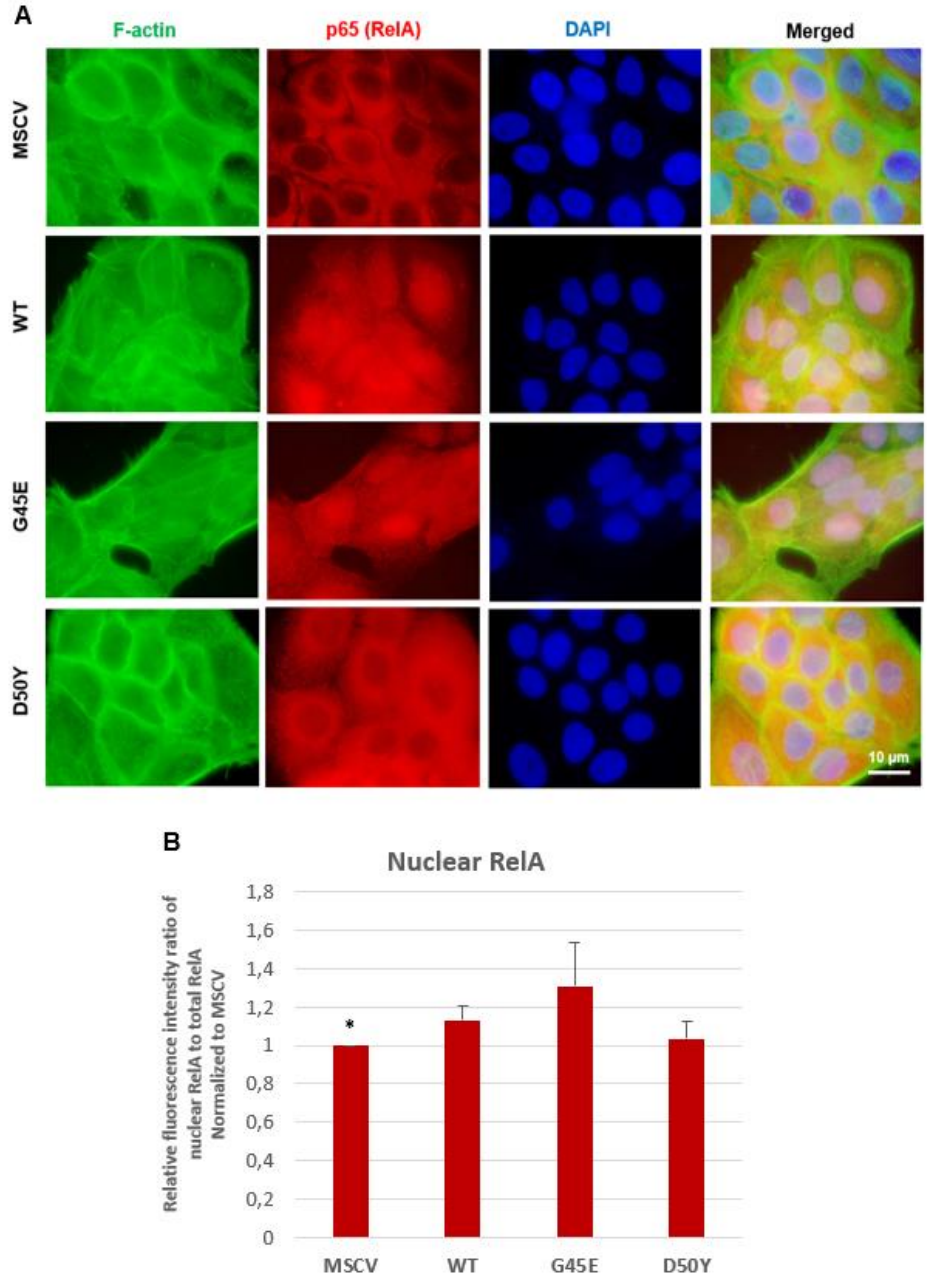

Figure 3.1.1 Immunostaining results of RelA (p65) protein. (A) Localization of RelA in MSCV, WT, G45E, D50Y cells. (B) The graph shows the relative fluorescence intensity ratio of nuclear RelA to total RelA protein in the cell with respect to MSCV. Images were taken at 100X (scale bar = 10 µm). Statistical significance was determined by unpaired t-test (n=4, ** $p < 0.05$). The error bars indicate the standard deviation.

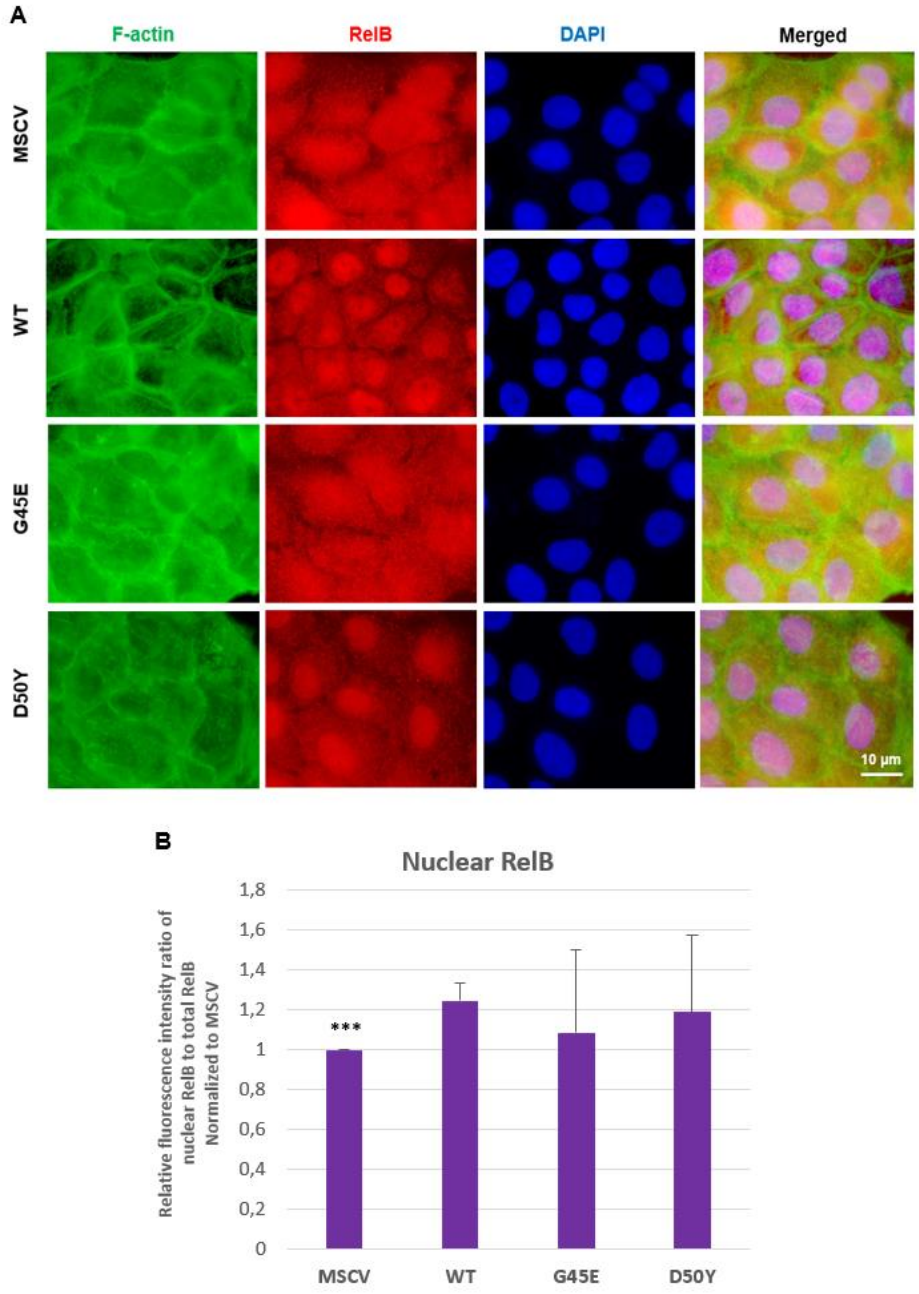

Figure 3.1.2 Immunostaining results of RelB protein. (A) Localization of RelB in MSCV, WT, G45E, D50Y cells. (B) The graph shows the relative fluorescence intensity ratio of nuclear RelB to total RelB protein in the cell with respect to MSCV. Images were taken at 100X (scale bar = 10 µm). Statistical significance was determined by unpaired t-test (n=4, *** $p < 0.005$). The error bars indicate the standard deviation.

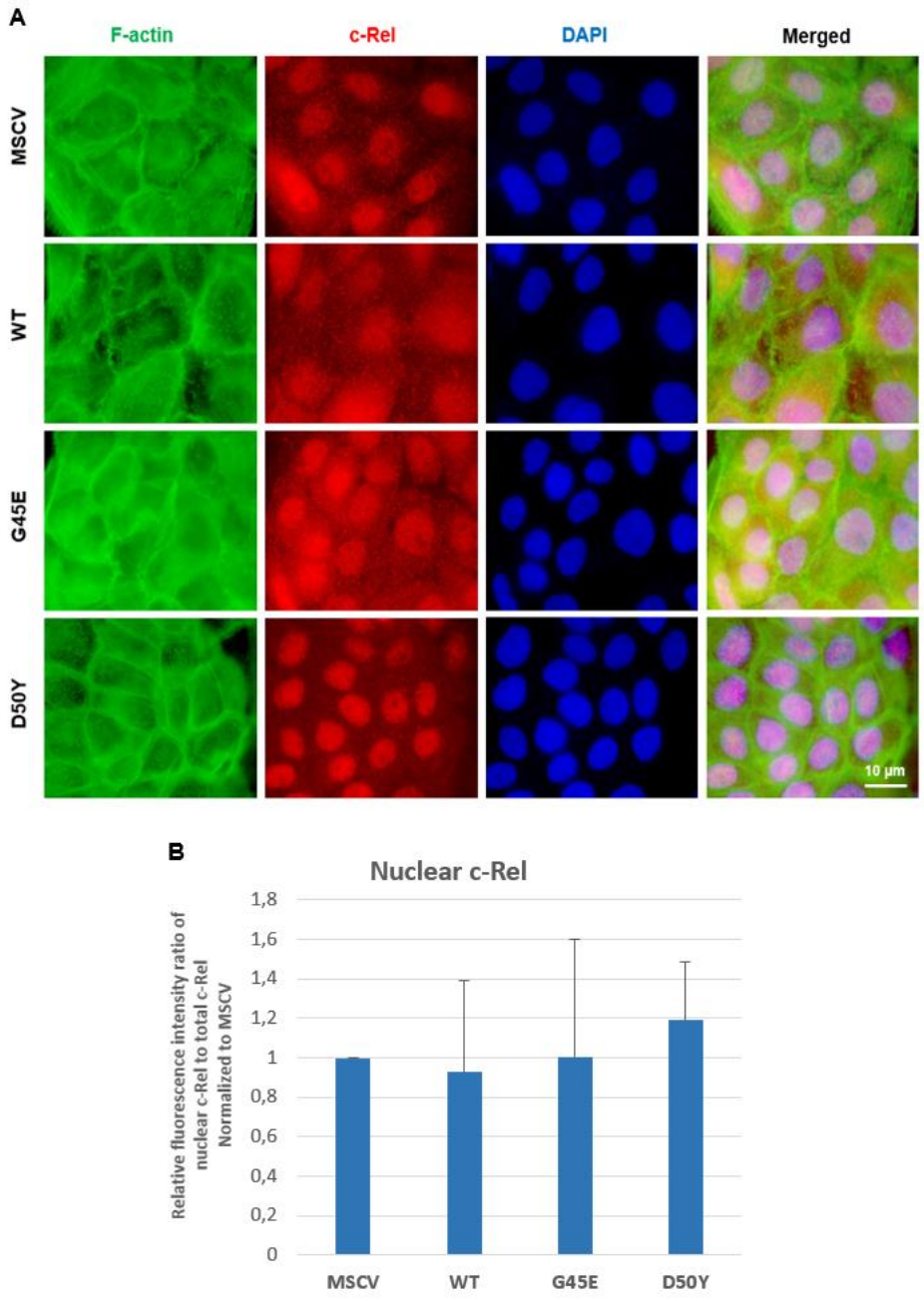

Figure 3.1.3 Immunostaining results of c-Rel protein. (A) Localization of c-Rel in MSCV, WT, G45E, D50Y cells. (B) The graph shows the relative fluorescence intensity ratio of nuclear c-Rel to total c-Rel protein in the cell with respect to MSCV. Images were taken at 100X (scale bar = 10 μm). Statistical significance was determined by unpaired t-test (n=3). The error bars indicate the standard deviation.

3.2 SECTION II

3.2.1 The effect of NF-κB on viability of HaCaT cells overexpressing WT Cx26 and KID Syndrome mutations G45E and D50Y.

To understand the effect of NF-κB on viability in HaCaT cells expressing WT, G45E, and D50Y constructs, MTT analysis was performed. First, different concentrations of NaSal (0.5 mM, 1 mM, and 2 mM) were tested to determine the optimum concentration that inhibits NF-κB pathway without killing the cells. The suitable NaSal concentration was determined to be 0.5 mM, which is the amount also used in the literature (Perugini et al., 2000), as 1 mM and 2 mM significantly decreased cell viability at the end of 7 days (Figure 3.2.1).

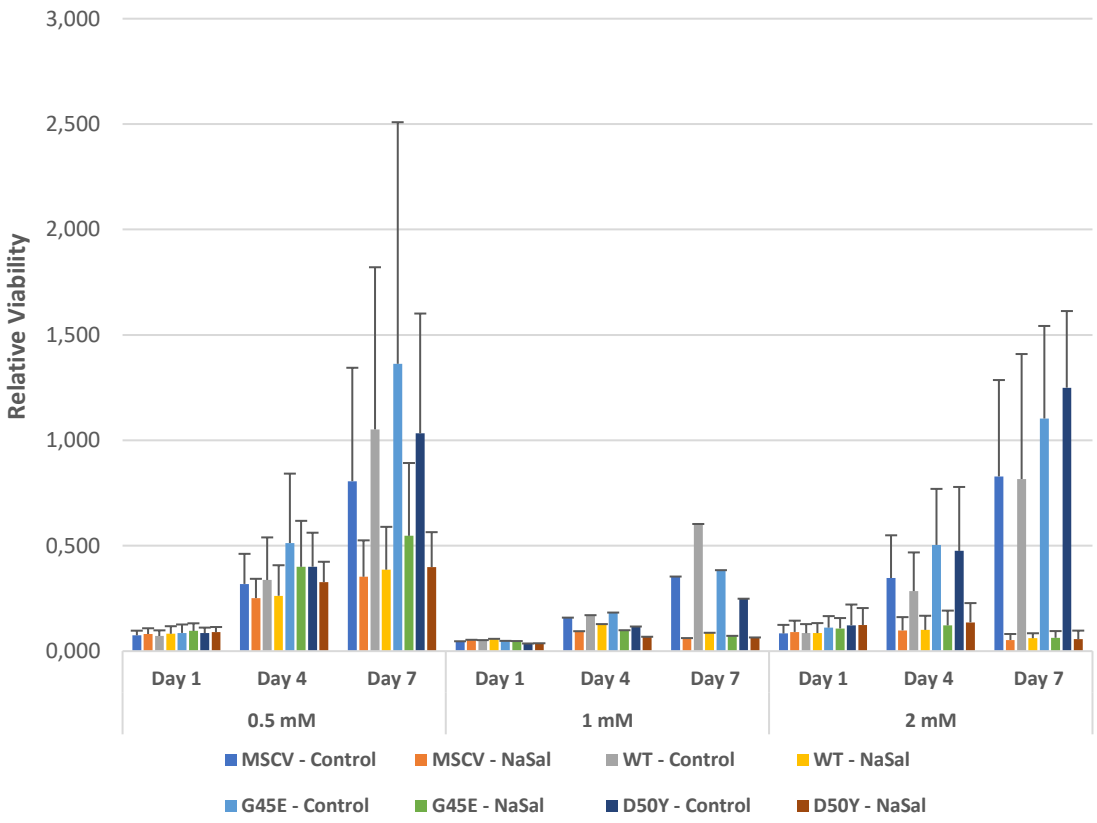

Figure 3.2.1 Spectrophotometric measurement of viable cells which were treated with 0.5 mM (n=4), 1 mM (n=1), 2 mM NaSal (n=4), and corresponding volume of dH_2O every 24 hours for 7 days. The error bars indicate the standard deviation.

After optimization experiments, cells were treated with 0.5 mM NaSal and corresponding volume of dH_2O for 7 days. The fold differences were determined by normalizing to the relative amount of control MSCV cells, which were treated with dH_2O. All cells treated with NaSal showed decreased viability after Day 1 compared to control groups (Figure 3.2.2). In both control and NaSal-treated groups, G45E showed the highest viability, followed by WT and D50Y, which were almost similar, while MSCV had the lowest viability (Figure 3.2.2).

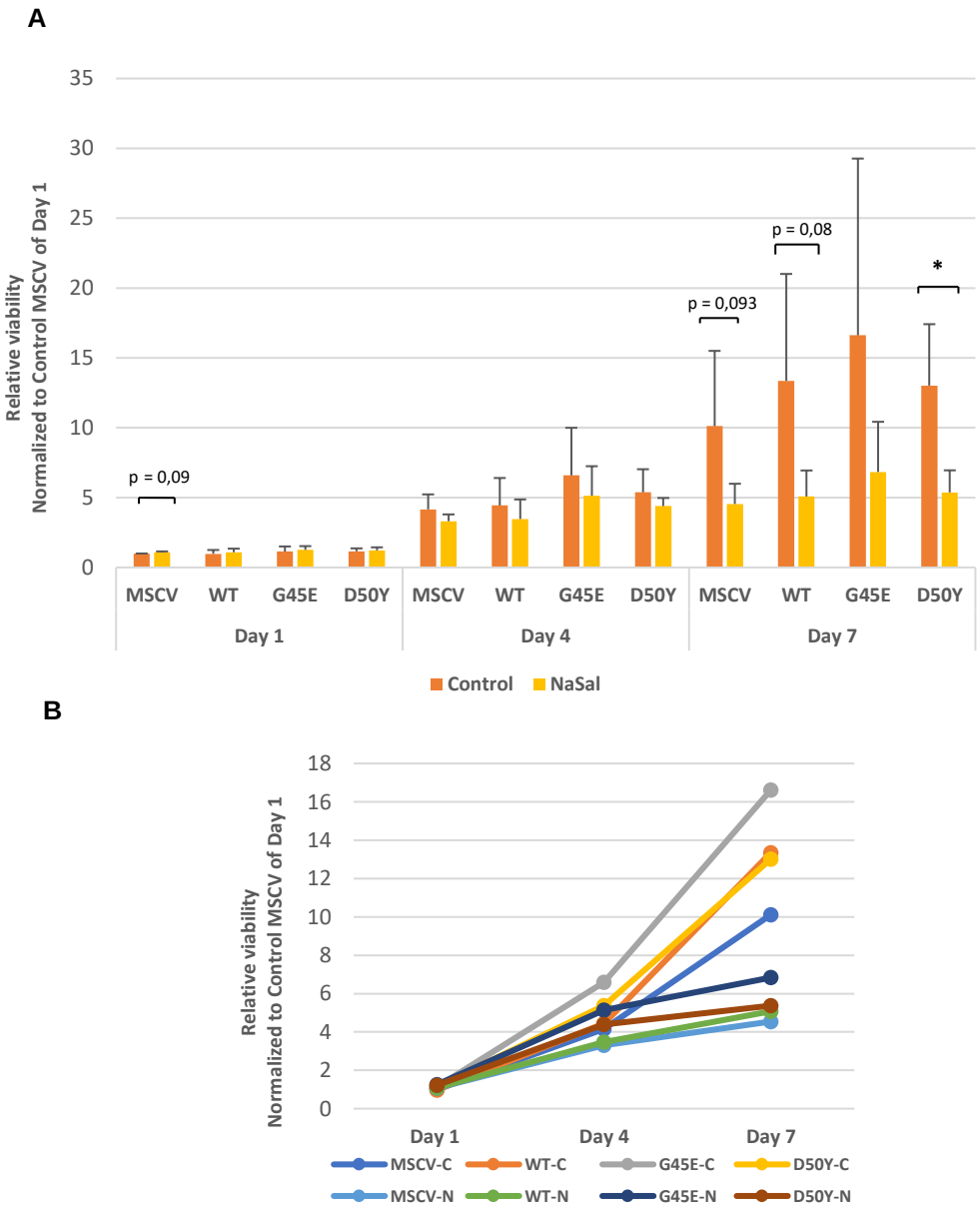

Figure 3.2.2 MTT analysis results that show (A) relative viability and (B) representative growth curve of MSCV, WT, G45E, and D50Y cells for day1, day4, and day7 with respect to control MSCV cells of day1. Cells were treated with dH_2O and 0.5 mM NaSal for every 24 hours. Statistical significance was determined by unpaired t-test (n=4, * $p < 0.05$). The error bars indicate the standard deviation.

KID syndrome variant Cx26-G45E generate hyperactive hemichannels that constantly open on the cell membrane, which results in cell lysis and death (Gerido et al., 2007). To understand the role of NF-κB on cell death in HaCaT cells expressing WT, G45E, and D50Y constructs, apoptosis analysis was performed. Cells were treated with 10 mM NaSal and corresponding volume of dH_2O for 6 hours. The fold differences were determined by normalizing to the relative amount of control MSCV cells, which were treated with dH_2O, in necrosis, late apoptosis, and early apoptosis. The fold differences in living cells were analysed in the same way.

After inhibition of NF-κB, necrosis and apoptosis (both early and late) decreased in WT, G45E and D50Y compared to control group. Additionally, MSCV showed significant decrease in early and late apoptosis rates after NaSal treatment. The difference between relative amount of living cells in control and NaSal-treated WT, G45E and D50Y were not significant, while MSCV showed significantly higher living cell ratio after treatment. Within control group, necrosis was 79% higher in D50Y and 43% higher in G45E compared to WT. Relative ratio of late apoptosis was the same for G45E and WT, while it was 22% higher in D50Y. In contrary, early apoptosis was 50% lower in D50Y and 53% higher in G45E compared to WT. There was no significant difference between WT, G45E, and D50Y in terms of living cells. Only, MSCV had significantly higher living cells ratio compared to WT (Figure 3.2.3). Within the NaSal-treated group, the G45E and D50Y mutations showed 29% and 53% higher necrosis, respectively, compared to WT. Relative ratio of late apoptosis was 13% higher in G45E compared to WT, while D50Y showed 65% higher ratio. On the other hand, G45E showed the highest ratio of early apoptosis among the NaSal-treated group, which is 49% higher than WT and 59% higher than D50Y. Moreover, D50Y significantly had the lowest early apoptosis ratio, being 40% lower than WT (Figure 3.2.3).

Figure 3.2.4 shows the sum of the percentages of early and late apoptosis raw data and indicates the total apoptosis percentages. Total apoptosis decreased in all the cells treated with 10 mM NaSal compared to control groups. Within control group, G45E showed the highest amount of apoptosis, followed by WT, D50Y, and MSCV, respectively. G45E cells showed a 22% higher rate of apoptosis compared to control WT cells, while D50Y cells exhibited a 13% lower rate. Within NaSal-treated group, similar to the control group, G45E showed the highest amount of apoptosis, whereas MSCV had the lowest. G45E cells showed a 34% higher rate of apoptosis compared to

control WT cells. On the other hand, D50Y cells exhibited almost similar rates of apoptosis with control WT cells, being only 3% higher (Figure 3.2.4).

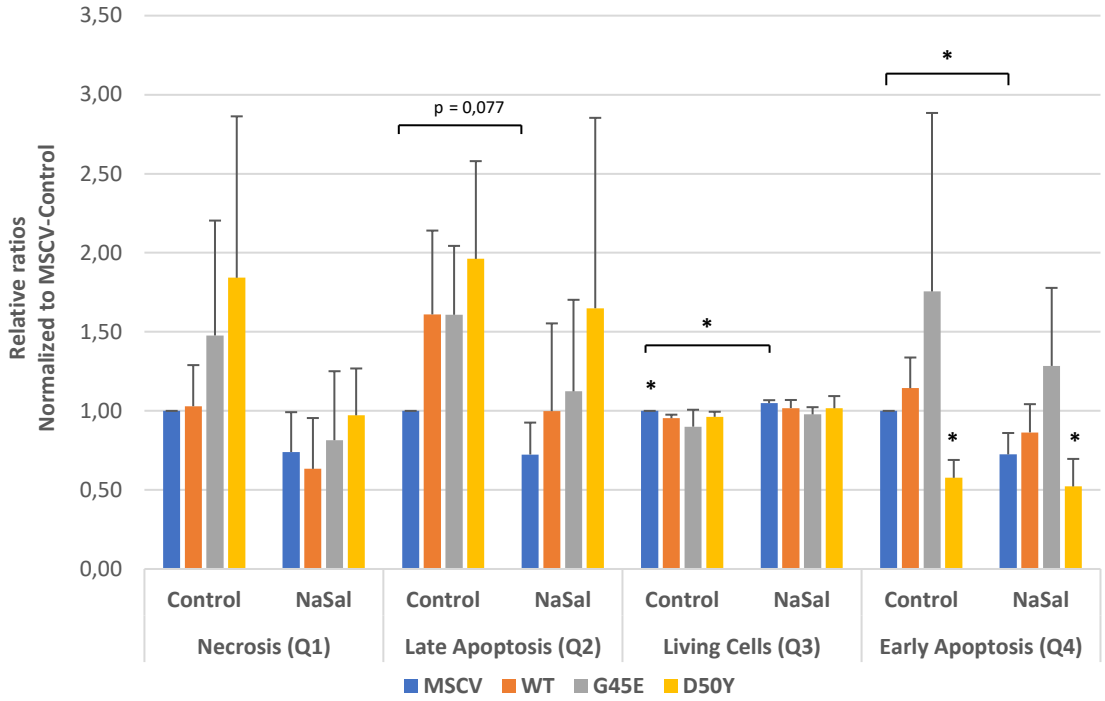

Figure 3.2.3 Relative ratios of MSCV, WT, G45E, and D50Y cells in necrosis, late apoptosis, living stage, and early apoptosis after dH_2O and 10 mM NaSal treatment with respect to control MSCV cells. Statistical significance was determined by unpaired t-test (n=3, * $p < 0.05$). The error bars indicate the standard deviation.

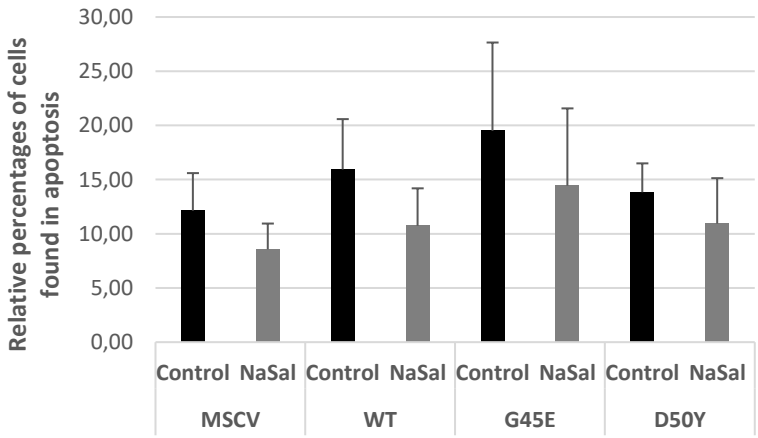

Figure 3.2.4 The sum of relative percentages of MSCV, WT, G45E, and D50Y cells in early and late apoptosis, indicating total apoptosis after dH_2O and 10 mM NaSal treatment (n=3). The error bars indicate the standard deviation.

3.3 SECTION III

3.3.1 The effect of NF-κB on proliferation of HaCaT cells overexpressing WT Cx26 and KID Syndrome mutations G45E and D50Y.

To understand the role of NF-κB on proliferation in HaCaT cells expressing WT, G45E, and D50Y constructs, BrdU assay was performed. Cells were treated with 10 mM NaSal and corresponding volume of dH_2O for 6 hours. Proliferation rate was determined by calculating proportion of BrdU-positive cells, indicating proliferative cells, to total number of cells. The fold differences were determined by normalizing to the ratio of control MSCV cells.

After NaSal treatment, MSCV showed a decrease in the relative number of proliferative cells (23% lower than control MSCV). There was almost no difference between control WT and NaSal-treated WT cells. NaSal-treated G45E also showed a decrease, being 31% lower than control G45E. NaSal-treated D50Y did not reveal a significant difference compared to control group (Figure 3.3.1).

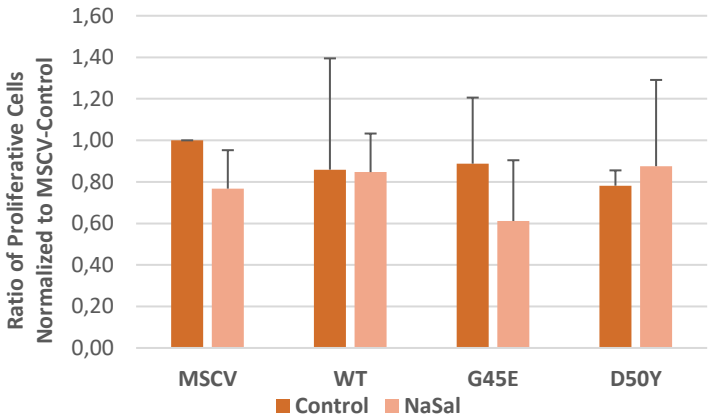

Figure 3.3.1 Ratio of proliferative cells to total cells for MSCV, WT, G45E, and D50Y after dH_2O and 10 mM NaSal treatment with respect to control MSCV cells (n=3). The error bars indicate the standard deviation.

Within control group, MSCV had the highest proliferation rate compared to WT, G45E, and D50Y. The proliferation rate was 12% higher in control G45E compared to

control D50Y. However, there was no significant difference between WT and KID syndrome mutants. In NaSal-treated cells, the trend was different. Similar to control group, NaSal-treated D50Y did not show a significant difference when compared with WT. On the other hand, G45E exhibited the lowest proliferation rate, with a 39% lower ratio than WT (Figure 3.3.1).

To understand the role of NF-κB in HaCaT cells expressing WT, G45E, and D50Y constructs, on proliferation, cell cycle analysis was also performed. Cells were treated with 10 mM NaSal and corresponding volume of dH_2O for 6 hours. The fold differences were determined by normalizing to the relative amount of control MSCV cells, which were treated with dH_2O, in G1, S, and G2 phases.

After treatment with NaSal, the relative number of control cells, except MSCV, undergoing G1 and S phases did not show a significant difference when compared with NaSal-treated group. On the other hand, in NaSal-treated cells in the G2 phase, MSCV exhibited a 18% decrease, WT showed a 14% decrease, G45E showed a 10% decrease, and D50Y showed a 14% decrease compared to their respective control groups (Figure 3.3.2).

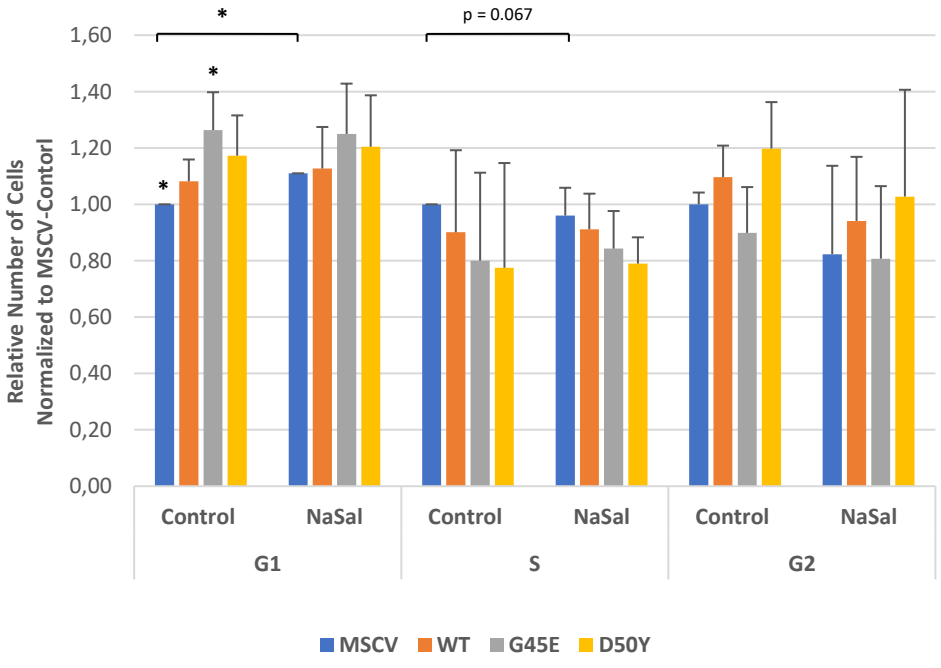

Figure 3.3.2 Relative number of MSCV, WT, G45E, and D50Y cells in the G1, S, and G2 phases, respectively, after dH_2O and 10 mM NaSal treatment with respect to control MSCV cells. Statistical significance was determined by unpaired t-test (n=5, * $p < 0.05$). The error bars indicate the standard deviation.

Among the control group, the percentage of G45E cells in the G1 phase was significantly 17% higher than WT, while D50Y cells were only 8% higher. In addition, the relative number of WT cells in G1 phase was significantly higher than MSCV in control group. On the other hand, both G45E and D50Y cells found in S phase were lower (11% and 14%, respectively) compared to WT. Additionally, control G45E cells in the G2 phase were 18% lower than WT in the control group. In contrast, D50Y cells showed a 9% increase compared to WT in the G2 phase (Figure 3.3.2). In the NaSal-treated group, G45E cells showed 11% higher ratio of cells compared to WT cells found in the G1 phase. Similarly, D50Y cells showed an increased ratio in the G1 phase, being 7% higher than WT. The percentage of G45E cells in the S phase was only 8% lower than WT, while D50Y cells were 13% higher. Finally, in the NaSal-treated group, D50Y cells in the G2 phase was 9% higher, whereas G45E cells were 14% lower compared to WT (Figure 3.3.2).

3.4 SECTION IV

3.4.1 The effect of NF-κB on differentiation of HaCaT cells overexpressing WT Cx26 and KID Syndrome mutations G45E and D50Y.

To understand the role of NF-κB on differentiation in HaCaT cells expressing WT, G45E, and D50Y constructs, expression levels of epidermal differentiation markers were measured by Q-RT PCR. Cells were treated with 10 mM NaSal and corresponding volume of dH_2O for 6 hours for inhibition of NF-κB pathway. TBP was used as a housekeeping gene, and mRNA levels for K14, involucrin, and K10 were normalized to TBP. The fold differences were determined by normalizing to the expression levels of control MSCV cells.

After treatment with NaSal, the expression levels of K14, a differentiation marker mainly expressed in the stratum basale, did not show a significant change in WT and G45E. On the other hand, NaSal-treated MSCV cells expressed 40% more K14, while expression levels decreased by 11% in NaSal-treated D50Y cells (Figure 3.4.1). In the control group, G45E and D50Y showed 35% and 48% higher K14 expression

levels, respectively, compared to WT. In the NaSal-treated group, the expression levels of K14 were almost the same for G45E and D50Y, and they exhibited approximately 32% more K14 expression than WT (Figure 3.4.1).

In addition to expression levels, protein levels of K14, K10, and involucrin were also investigated in WT, G45E, and D50Y by Western blotting (only for K14) and immunostaining. Similarly, the cells were treated with 10 mM NaSal and corresponding volume of dH_2O for 6 hours for inhibition of NF-κB pathway. In Western blotting, the relative K14 protein levels were normalized to the β-actin protein in the cells.

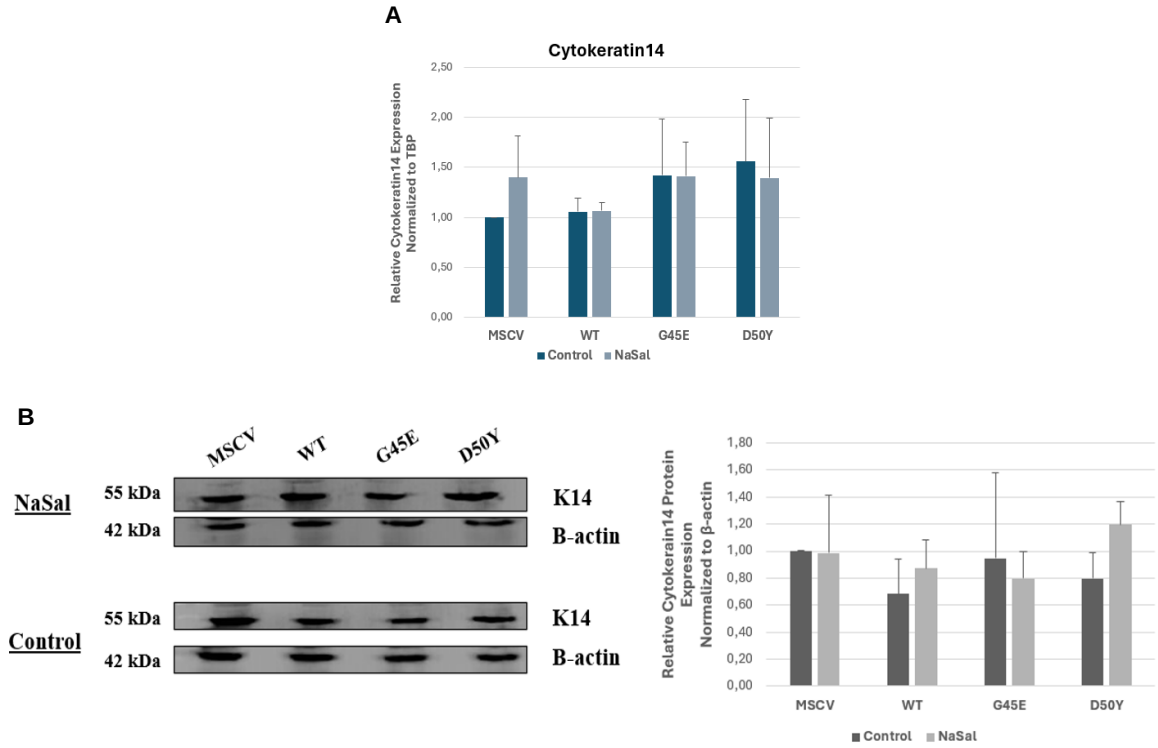

Figure 3.4.1 Relative K10 (A) mRNA expression and (B) protein levels in WT, G45E, and D50Y cells after dH_2O and 10 mM NaSal treatment with respect to control MSCV cells. Statistical significance was determined by unpaired t-test. The error bars indicate the standard deviation.

According to the Western blotting results, K14 protein level increased 28% in WT after NaSal treatment, while it decreased by 16% in G45E. In addition, NF-κB inhibition increased K14 protein levels in D50Y. Finally, MSCV did not affected by NaSal treatment. Within control group, WT had the lowest K14 protein level, whereas G45 had the highest. D50Y had 17% higher K14 protein compared to WT. Within

NaSal-treated group, trend was different. D50Y had the highest K14 protein level, while G45E had the lowest in this case. NaSal-treated WT and G45E did not show a prominent difference.

In immunostaining experiments, the proportion of total fluorescence signal of the corresponding protein to the number of cells was calculated for verification. The fold differences were determined by normalizing to the relative fluorescence intensity of control MSCV cells.

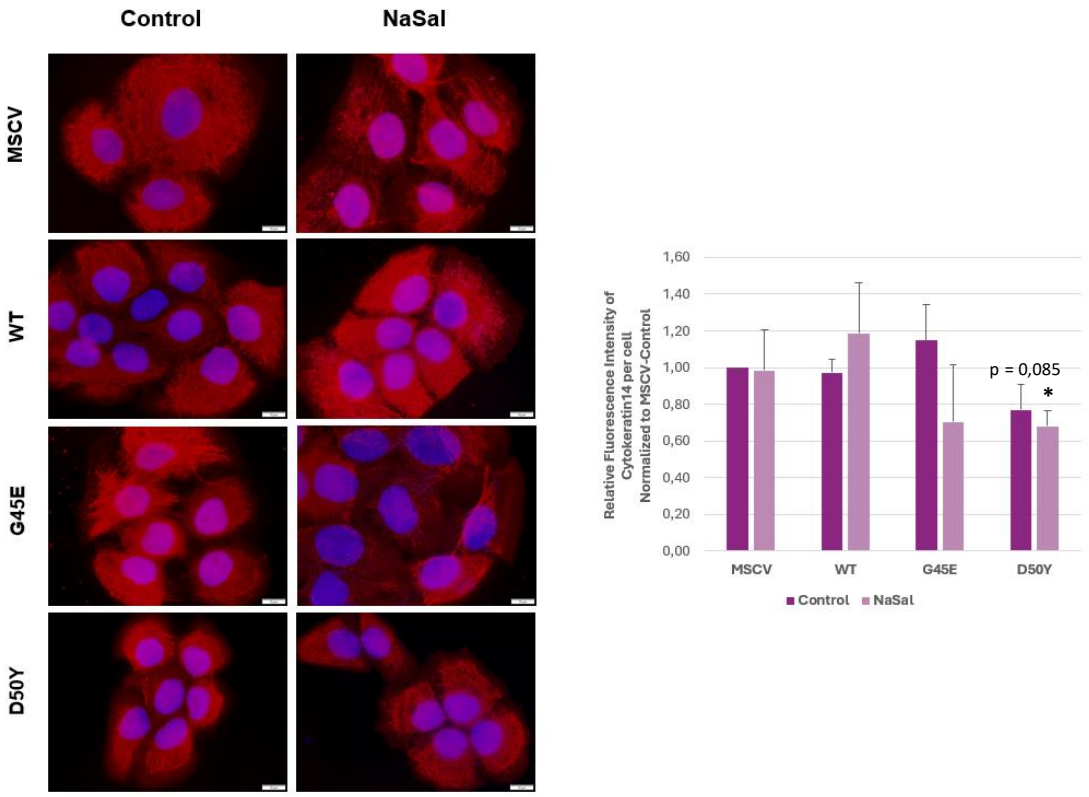

Figure 3.4.2 Relative fluorescence intensity of cytokeratin14 protein per cell with respect to control MSCV cells. Images were taken at 100X (scale bar = 10 µm). Statistical significance was determined by unpaired t-test (n=3, * $p < 0.05$). The error bars indicate the standard deviation.

NaSal treatment of the cells caused 22% increase in K14 protein levels of WT, while protein levels of G45E decreased by 39% compared to the corresponding control cells, showing similar trend with Western blotting results (Figure 3.4.1 & Figure 3.4.2). On the contrary, K14 protein level decreased by 12% in D50Y compared to control D50Y (Figure 3.4.2).

Within the control group, G45E had the highest K14 signal, consistent with Western blotting (Figure 3.4.1 & Figure 3.4.2). K14 levels of control G45E were 18% higher compared to control WT, and D50Y showed 21% lower protein levels. In the NaSal-treated group, WT had the highest K14 levels. G45E and D50Y had almost similar levels, being approximately 41-43% lower than WT (Figure 3.4.2).

Involucrin is considered as an intermediate differentiation marker as mentioned. After inhibition of NF-κB, the mRNA expression levels of involucrin did not change significantly (Figure 3.4.3). In the control group, D50Y exhibited the greatest expression, being 3.8-fold higher than WT and 1.5-fold higher than G45E. Compared to control WT, G45E showed 90% higher involucrin expression levels. In the NaSal-treated group, involucrin mRNA levels were higher by approximately 51% in G45E and by about 250% in D50Y when compared with WT (Figure 3.4.3).

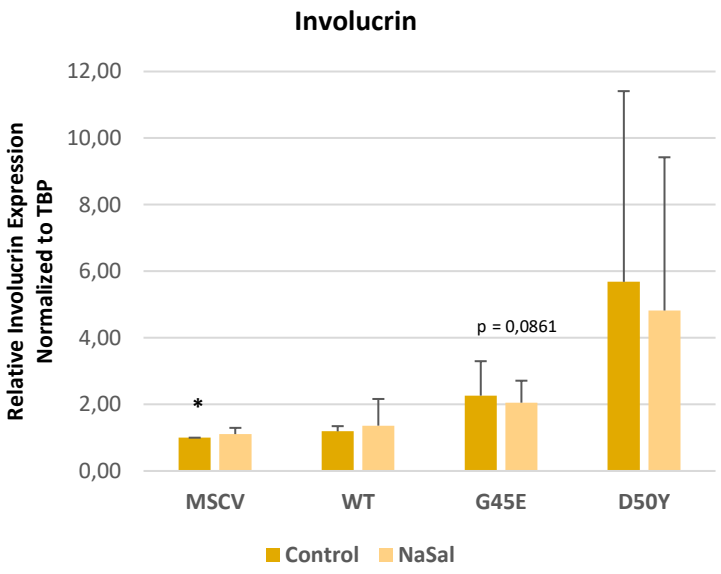

Figure 3.4.3 Relative involucrin mRNA expression levels in WT, G45E, and D50Y cells after dH_2O and 10 mM NaSal treatment with respect to control MSCV cells. Statistical significance was determined by unpaired t-test (n=4, * $p < 0.05$). The error bars indicate the standard deviation.

NaSal treatment increased involucrin protein levels in all groups. Within the control group, protein levels of D50Y were 28% lower compared to WT. Control G45E did not show a difference when compared with WT. In the NaSal-treated group, WT

exhibited the highest involucrin protein levels, being 13% and 7% higher than G45E and D50Y, respectively. Involucrin protein signal was 28% higher in control G45E compared to control D50Y, while NaSal-treated G45E and D50Y did not show a prominent difference (Figure 3.4.4).

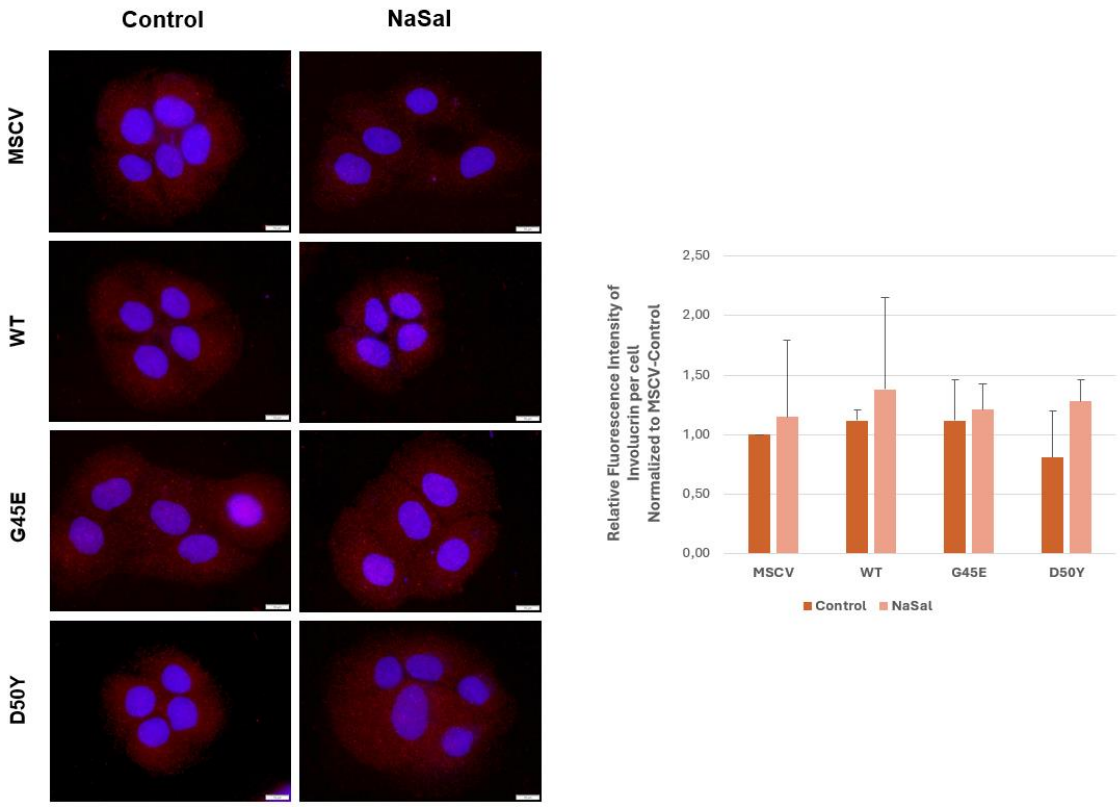

Figure 3.4.4 Relative fluorescence intensity of involucrin protein per cell with respect to control MSCV cells. Images were taken at 100X (n=3; scale bar = 10 µm). Statistical significance was determined by unpaired t-test. The error bars indicate the standard deviation.

K10 is one of the proteins highly expressed in stratum spinosum during epidermal differentiation. When the cells were treated with NaSal, all of them exhibited decreased K10 expression (Figure 3.4.5). In the control group, G45E and D50Y showed higher K10 expression, approximately 1.8-fold greater than WT. Similarly, NaSal-treated G45E and D50Y showed increased K10 expression, being 154% higher in G45E and 223% higher in D50Y compared to WT (Figure 3.4.5).

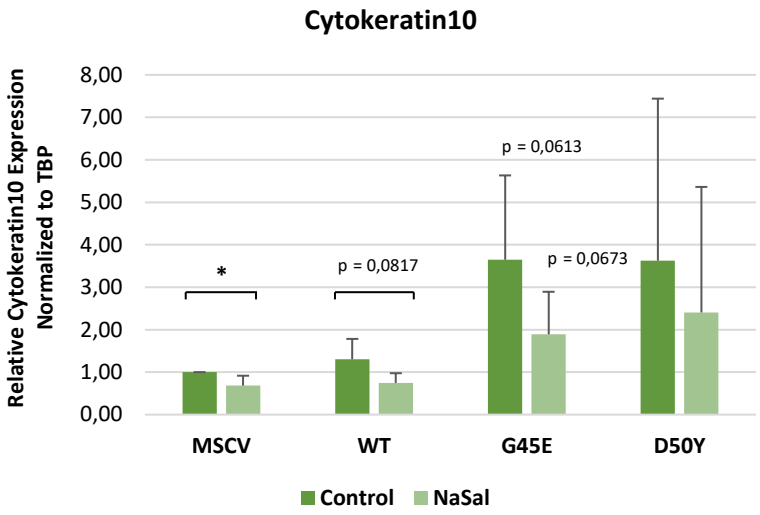

Figure 3.4.5 Relative K10 mRNA expression levels in WT, G45E, and D50Y cells after dH_2O and 10 mM NaSal treatment with respect to control MSCV cells. Statistical significance was determined by unpaired t-test (n=4, * $p < 0.05$). The error bars indicate the standard deviation.

NaSal treatment of the cells caused 24% and 12% decrease K10 protein levels in G45E and D50Y, respectively, compared to the corresponding control cells. NaSal-treated MSCV and WT showed significant decrease compared to control MSCV and WT, respectively. Within the control group, protein levels of G45E were 48% higher compared to WT. Control D50Y also showed increased protein levels, being 24% higher than control WT. Similarly, mutant cells had the highest K10 levels in the NaSal-treated group. NaSal-treated G45E and D50Y had almost similar levels, being approximately 8-11% higher than NaSal-treated WT. Inhibition of NF-κB brought the protein levels of G45E and D50Y closer to those of WT. (Figure 3.4.6).

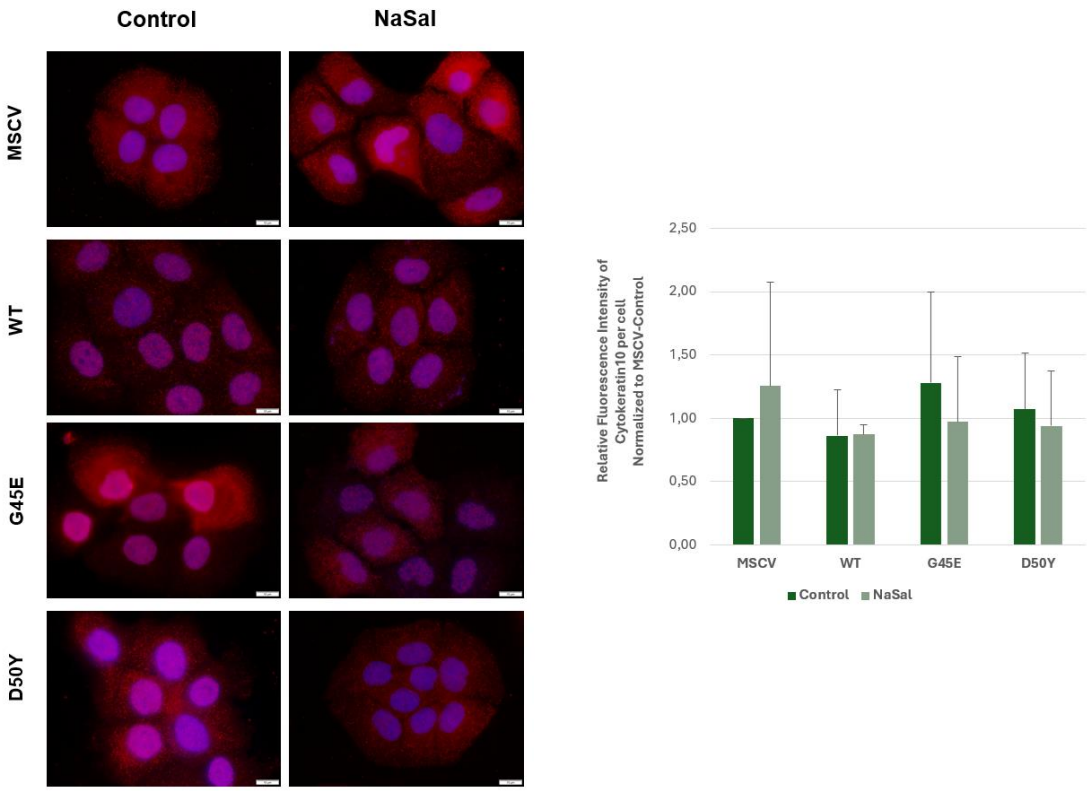

Figure 3.4.6 Relative fluorescence intensity of cytokeratin10 protein per cell with respect to control MSCV cells. Images were taken at 100X (scale bar = 10 µm). Statistical significance was determined by unpaired t-test (n=3). The error bars indicate the standard deviation.

CHAPTER 4

DISCUSSION AND CONCLUSION

In this study, the effects of the NF-κB signaling pathway on the proliferation and differentiation mechanisms of the HaCaT keratinocyte cell lines which constitutively express Cx26 WT and KID syndrome mutations (Cx26-G45E and Cx26-D50Y) were investigated. Cx26 KID syndrome mutations lead to distinct symptoms and phenotypes with varying severity in patients (Meigh et al., 2014). For example, Cx26-G45E causes lethality in affected individuals (Lilly et al., 2019), whereas Cx26-D50Y results in milder symptoms as mentioned previously (Yotsumoto et al., 2003; Arndt et al., 2010; Aypek et al., 2016). Both mutations cause formation of hyperactive hemichannels on the cell membrane. These “leaky” hemichannels result in uncontrolled molecule transfer and disrupt epidermal homeostasis by affecting the proliferation and differentiation of keratinocytes. However, the exact molecular and cellular mechanisms underlying the epidermal alterations observed in Cx26 mutations-induced KID syndrome are not known yet. Based on the literature, NF-κB family have important roles in proliferation and differentiation of keratinocytes (Bell et al., 2003; Gugasyan et al., 2004; Zhang et al., 2017). Some of the studies revealed contradictory results, highlighting the complexity of the mechanism by which NF-κB regulates epidermopoiesis (Bell et al., 2003). Therefore, it is hypothesized that mutant Cx26 channels may result in epidermal diseases by altering proliferation and differentiation mechanisms of keratinocytes via NF-κB pathway.

In the first part of the study, the activity of NF-κB pathway was investigated in cells carrying KID syndrome mutations. NF-κB members are normally found inactive in the cytoplasm. Upon activation of the pathway, NF-κB transcription factors, RelA, RelB, or c-Rel, translocate to the nucleus. In the nucleus, they can induce or repress the expression of specific target genes (Guo et al., 2024). Localization analysis of RelA showed cytosolic localization in D50Y, while G45E revealed the highest nuclear fluorescence signal compared to the others. Active NF-κB/RelA significantly upregulated in the epidermis of psoriatic plaques (Takao et al., 2003; Lizzul et al.,

2005), which may explain high nuclear RelA signal in G45E. Previous studies showed that D50Y causes hyperproliferation (Aypek et al., 2016). Skin cells of mice overexpressing active p65 had almost no DNA synthesis, indicating inhibition in proliferation (Seitz et al., 1998), consistent with the reduced nuclear activity of RelA in hyperproliferative KID syndrome mutant D50Y. In addition, WT had significantly higher nuclear RelA signal. In the normal epidermis, NF-κB is constitutively expressed in a nonactivated (cytoplasmic) state. Higher NF-κB/RelA activity in WT may be caused by Cx26 overexpression.

Nuclear RelB signal did not show a significant difference in both KID syndrome mutations compared to WT, suggesting that non-canonical NF-κB pathway may not be activated in Cx26 KID syndrome mutations. However, WT had a significantly higher nuclear RelB signal compared to MSCV. Similar to RelA, the overexpression of Cx26 in WT may be the underlying reason for this increase. Peptidoglycan (PGN) *from S. aureus* induced TLR2 expression in HaCaT keratinocyte cells, and TLR2 induced upregulation of Cx26 via NF-κB (García-Vega et al., 2019). Significant increase NF-κB/RelA and NF-κB/RelB activity in WT, which overexpress Cx26, compared to MSCV may be explained by this finding.

Nuclear localization of c-Rel was highest in D50Y compared to WT, while G45E did not exhibit a prominent difference. Keratinocytes of c-Rel deficient mice had reduced proliferation (Fullard et al., 2013). Another study demonstrated that downregulation of c-Rel increased apoptosis and reduced keratinocyte proliferation (Lorenz et al., 2015). These findings suggested that c-Rel has role in regulating keratinocyte proliferation and homeostasis, consistent with increased nuclear activity of c-Rel in keratinocytes expressing hyperproliferative D50Y mutation.

The effect of NF-κB on viability in WT, G45E, and D50Y was investigated by MTT analysis. NaSal treatment decreased cell viability in all groups. The trend was the same for both control and NaSal-treated groups. NF-κB can activate innate immunity and inflammation, inhibit apoptosis, and increase cell proliferation (Serasanambati & Chilakapati, 2016). Reduced viability of WT, G45E, and D50Y after NF-κB inhibition may be explained by that. Nevertheless, KID syndrome variant G45E showed a difference compared to WT and D50Y with the highest viability at the end of 7 days. Consistently, Cx26-G45E mice showed increased epidermal cell proliferation (Mese et

al., 2011), indicating that the cells divide and raise their numbers. This may explain the high viability of keratinocytes expressing G45E construct. WT and D50Y exhibited almost the same viability at the end of 7 days. Since D50Y does not have lethal effects (Aypek et al., 2016), similar viability ratios with WT may be expected. On the other hand, NF-κB inhibition decreased the relative viability of all cells in both the control and NaSal-treated groups by 59-60%, suggesting that the underlying mechanism of proliferation in KID syndrome mutants may not be regulated by the NF-κB pathway.

The role of NF-κB on proliferation of HaCaT cells expressing WT, G45E, and D50Y constructs was investigated by performing BrdU assay, which is used to detect cell proliferation by measuring DNA synthesis, particularly identifying cells in the S phase. Cx26-G45E mice revealed increased cell proliferation in the epidermis related to raised hemichannel current due to mutation (Mese et al., 2011; Peres et al., 2023). Consistent with MTT analysis, control G45E showed higher proliferation rate compared to control D50Y. After treatment with NaSal, the relative ratio of proliferative G45E cells decreased, while WT did not exhibit a significant difference, suggesting a role of NF-κB pathway on proliferation mechanisms of HaCaT cells expressing G45E mutation.

Several studies suggested a coordination between the cell cycle and NF-κB activation. NF-κB can activate the transcription of a key positive regulator of the G1 to S phase progression. Inhibition of NF-κB resulted in delayed cell-cycle progression (Barkett & Gilmore, 1999). Consistent with this, NaSal treatment increased the relative number of cells in G1 phase and decreased those in S phase. Furthermore, the relative number of G45E cells in S phase, in which DNA replication occurs (Fischer et al., 2018), was higher than D50Y, consistent with the results of MTT and BrdU analysis. NF-κB also have role in G2/M regulation (Ledoux & Perkins, 2014). However, NF-κB inhibition did not affect KID syndrome mutants differently than WT, indicating that NF-κB may not affect cell cycle mechanisms of HaCaT cells based on KID syndrome mutants.

As mentioned previously, Cx26-G45E generate hyperactive hemichannels on the cell membrane, causing cell lysis and death (Gerido et al., 2007). To understand the role of NF-κB on cell death in KID syndrome variants Cx26-G45E and Cx26-D50Y, apoptosis analysis was also performed. Total apoptosis rates decreased in NaSal-treated

WT, G45E, and D50Y compared to the control group. NF-κB has significant roles in protection of keratinocytes against apoptosis in homeostatic and inflammatory conditions (Lippens et al., 2009). On the other hand, several studies suggested that the activation of NF-κB can make some cells more susceptible to apoptosis-inducing agents which work through or along with the Fas pathway. This can occur since NF-κB can activate the genes encoding Fas ligand or the Fas receptor (Matsui et al., 1998; Barkett & Gilmore, 1999; Kasibhatla et al., 1999). This may explain decreased apoptosis rates in all groups after inhibition of NF-κB by sodium salicylate. G45E showed the highest total apoptosis rates compared to WT and D50Y, which had nearly identical total apoptosis rates, consistent with the lethal nature of G45E mutation (Lilly et al., 2019). WT had higher total apoptosis rates compared to MSCV in both control and NaSal-treated groups (Figure 3.2.4). Also, MSCV had significantly higher relative living cell ratio compared to WT according to the apoptosis analysis (Figure 3.2.3), consistent with BrdU analysis which showed higher proliferation rate in control MSCV compared to control WT (Figure 3.3.1). Overexpression of Cx26 decreased Bcl-2 expression and induced apoptosis in three different human prostate cancer cell lines (Tanaka & Grossman, 2004). Another study showed that knocking down of Cx26 in human skin squamous cell carcinoma cells reduced expression of ERK, which has important roles in apoptosis (Sun et al., 2021). Increased total apoptosis rates and lower living cell ratio in Cx26-overexpressing WT group compared to MSCV may be consistent with these findings.

NF-κB transcription factors are considered as main regulators of programmed cell death through apoptosis or necrosis (Dutta et al., 2006). Necrosis decreased after NaSal treatment, indicating that NF-κB plays a role in the regulation of necrosis in the cell. However, KID syndrome mutants did not show a significant difference in the relative amount of necrosis when they were compared with WT. Apoptosis can take place either before the first mitosis (early apoptosis) or as the final stage of mitotic catastrophe (late apoptosis) (Alphonse et al., 2013). D50Y exhibited the highest late apoptosis rates and significantly the lowest early apoptosis rates in both control and NaSal-treated groups. On the contrary, G45E showed the lowest late apoptosis rates and the highest early apoptosis rates, suggesting NF-κB may affect apoptosis through different mechanisms in KID syndrome mutants. Although all the cells showed a decrease in the relative early and late apoptosis rates after NF-κB inhibition, NaSal

treatment affected these rates differently in D50Y, indicating the effect of NF-κB on apoptosis mechanisms of KID syndrome mutant.

Only basal keratinocytes can proliferate and differentiate into mature cells to form the cornified layers. However, the control of genes that regulate terminal differentiation is not yet fully understood. Several studies indicate that NF-κB, or elements of the system (e.g., IKKα), appear to play a role in the development and differentiation of the epidermis (Bell et al., 2003). In the last part of the study, the role of NF-κB on differentiation of HaCaT cells expressing WT, G45E, and D50Y constructs was investigated by measuring mRNA expression and protein levels of epidermal differentiation markers, K14, involucrin, and K10 after inhibition of NF-κB pathway. The highest K14 mRNA expression level was observed in D50Y followed by G45E and WT, respectively, in both control and NaSal-treated groups. K14 is mainly expressed in proliferative basal keratinocytes (Peres et al., 2023), which may explain high K14 expression in hyperproliferative D50Y. Both K14 mRNA and protein levels were also higher in G45E compared to WT. Cx26-G45E mice showed increased epidermal cell proliferation (Mese et al., 2011), consistent with this finding. The mRNA expression levels of K14 in WT and G45E did not change significantly after NaSal treatment, while it was downregulated by 11% in D50Y, suggesting a role of NF-κB on differentiation mechanism of HaCaT cells expressing D50Y mutation.

Differentiated keratinocytes of the suprabasal layers predominantly express K10 and downregulate expression of K14 (Figure 1.1) (Peres et al., 2023). In both control and NaSal-treated groups, K10 was significantly upregulated in G45E compared to WT, suggesting increased differentiation in G45E. Immunostaining results, showing relative amount of K10 protein in cells, were also consistent with Q RT-PCR results. G45E showed higher K10 protein levels compared to WT. NF-κB inhibition decreased both mRNA and protein levels of K10 in G45E, while NaSal-treatment did not have a prominent effect on K10 protein levels of WT cells, suggesting that NF-κB may have role in differentiation mechanisms of HaCaT cells expressing G45E mutation. As mentioned above, IKKα-deficient mice had failed activation of NF-κB, and also prevented terminal differentiation in epidermal keratinocytes (Hu et al., 2001), consistent with the finding of downregulation and decreased protein levels of K10 after NaSal treatment.

Involucrin is expressed in nonkeratinized corneal epithelium, and it is considered as an intermediate differentiation marker (Rousselle et al., 2017). Involucrin mRNA expression significantly upregulated in control G45E compared to control WT, while control MSCV had significantly lower mRNA expression. Cx26 overexpression and mutation may be the reason for increased differentiation in WT and G45E cells, respectively. However, NaSal treatment did not affect involucrin mRNA expression or protein levels significantly in mutant cells. Since involucrin is expressed mostly in suprabasal layers, 2D cell culture may not be sufficient to observe alterations in this differentiation marker. 3D cell culture or a transgenic mice model may be more useful to examine the effect better.

In conclusion, G45E and D50Y cells showed NF-κB activity through different NF-κB members, which are RelA and c-Rel, respectively. In addition, Cx26 overexpression significantly increases NF-κB activity through RelA and RelB. Furthermore, NF-κB may affect apoptosis in G45E and D50Y through different mechanisms and may have effect on early and late apoptosis mechanisms of D50Y. Finally, NF-κB may have role in regulating proliferation and differentiation mechanisms of G45E.

REFERENCES

Abdo, Joseph M., Nikolai A. Sopko, and Stephen M. Milner. 2020. “The Applied Anatomy of Human Skin: A Model for Regeneration.” *Wound Medicine*. Elsevier GmbH. https://doi.org/10.1016/j.wndm.2020.100179.

Abhishek, Sinha, and Suresh Palamadai Krishnan. 2016. “Epidermal Differentiation Complex: A Review on Its Epigenetic Regulation and Potential Drug Targets.” *Cell Journal* 18 (1): 1–6. https://doi.org/https://doi.org/10.22074/cellj.2016.3980.

Alphonse, Gersende, Mira Maalouf, Priscillia Battiston-Montagne, Dominique Ardail, Michaël Beuve, Robert Rousson, Gisela Taucher-Scholz, Claudia Fournier, and Claire Rodriguez-Lafrasse. 2013. “P53-Independent Early and Late Apoptosis Is Mediated by Ceramide after Exposure of Tumor Cells to Photon or Carbon Ion Irradiation.” *BMC Cancer* 13 (1): 151. https://doi.org/10.1186/1471-2407-13-151.

Anderton, Holly, and Suhaib Alqudah. 2022. “Cell Death in Skin Function, Inflammation, and Disease.” *Biochemical Journal*. Portland Press Ltd. https://doi.org/10.1042/BCJ20210606.

Arndt, Susan, Antje Aschendorff, Christian Schild, Rainer Beck, Wolfgang Maier, Roland Laszig, and Ralf Birkenhäger. 2010. “A Novel Dominant and a De Novo Mutation in the GJB2 Gene (Connexin-26) Cause Keratitis-Ichthyosis-Deafness Syndrome.” *Otology & Neurotology* 31 (2): 210–15. https://doi.org/10.1097/MAO.0b013e3181cc09cd.

Avshalumova, Lyubov, Jordan Fabrikant, and Angie Koriakos. 2014. “Overview of Skin Diseases Linked to Connexin Gene Mutations.” *International Journal of Dermatology* 53 (2): 192–205. https://doi.org/10.1111/ijd.12062.

Aypek, Hande, Veysel Bay, and Gülistan Meşe. 2016. “Altered Cellular Localization and Hemichannel Activities of KID Syndrome Associated Connexin26 I30N and D50Y Mutations.” *BMC Cell Biology* 17 (1). https://doi.org/10.1186/s12860-016-0081-0.

Barbieri, J. S., K. Wanat, and J. Seykora. 2014. “Skin: Basic Structure and Function.” In *Pathobiology of Human Disease: A Dynamic Encyclopedia of Disease Mechanisms*, 1134–44. Elsevier Inc. https://doi.org/10.1016/B978-0-12-386456-7.03501-2.

Barkett, Margaret, and Thomas D Gilmore. 1999. “Control of Apoptosis by Rel/NF-KB Transcription Factors.” *Oncogene* 18 (49): 6910–24. https://doi.org/10.1038/sj.onc.1203238.

Barton, Debra, Harm HogenEsch, and Falk Weih. 2000. “Mice Lacking the Transcription Factor RelB Develop T Cell-Dependent Skin Lesions Similar to Human Atopic Dermatitis.” *European Journal of Immunology* 30 (8): 2323–32. https://doi.org/10.1002/1521-4141(2000)30:8<2323::AID-IMMU2323>3.0.CO;2-H.

Bell, Susanne, Klaus Degitz, Martina Quirling, Nikolaus Jilg, Sharon Page, and Korbinian Brand. 2003. “Involvement of NF-KB Signalling in Skin Physiology and Disease.” *Cellular Signalling* 15 (1): 1–7. https://doi.org/10.1016/S0898-6568(02)00080-3.

Ben-Neriah, Yinon, and Michael Karin. 2011. “Inflammation Meets Cancer, with NF-KB as the Matchmaker.” *Nature Immunology* 12 (8): 715–23. https://doi.org/10.1038/ni.2060.

Brown, Keith D, Estefania Claudio, and Ulrich Siebenlist. 2008. “The Roles of the Classical and Alternative Nuclear Factor-KappaB Pathways: Potential Implications for Autoimmunity and Rheumatoid Arthritis.” *Arthritis Research & Therapy* 10 (4): 212. https://doi.org/10.1186/ar2457.

Boulais, Nicholas, and Laurent Misery. 2008. “The Epidermis: A Sensory Tissue.” *European Journal of Dermatology: EJD* 18 (2): 119–27. https://doi.org/https://doi.org/10.1684/ejd.2008.0348.

Burns, FS. 1915. “A Case of Generalized Congenital Keratoderma with Unusual Involvement of the Eyes, Ears, and Nasal and Buccous Membranes.” *Journal of Cutaneous Diseases* 33: 255–60.

Caceres-Rios, Hector, Lourdes Tamayo-Sanchez, Carola Duran-Mckinster, Ma. de la Luz Orozco, and Ramon Ruiz-Maldonado. 1996. “Keratitis, Ichthyosis, and Deafness (KID Syndrome): Review of the Literature and Proposal of a New Terminology.” *Pediatric Dermatology* 13 (2): 105–13. https://doi.org/10.1111/j.1525-1470.1996.tb01414.x.

Cammarata-Scalisi, Francisco, Colin Eric Willoughby, Antonio Cárdenas Tadich, Nancy Labrador, Adriana Herrera, and Michele Callea. 2020. “Clinical, Etiopathogenic, and Therapeutic Aspects of KID Syndrome.” *Dermatologic Therapy* 33 (4). https://doi.org/10.1111/dth.13507.

Cao, Fengli, Reiner Eckert, Claudia Elfgang, Johannes M. Nitsche, Scott A. Snyder, Dieter F. Hülser, Klaus Willecke, and Bruce J. Nicholson. 1998. “A Quantitative Analysis of Connexin-Specific Permeability Differences of Gap Junctions Expressed in HeLa Transfectants and X *Enopus* Oocytes.” *Journal of Cell Science* 111 (1): 31–43. https://doi.org/10.1242/jcs.111.1.31.

Chanson, Marc, Masakatsu Watanabe, Erin M. O’Shaughnessy, Alice Zoso, and Patricia E. Martin. 2018. “Connexin Communication Compartments and Wound Repair in Epithelial Tissue.” *International Journal of Molecular Sciences* 19 (5). https://doi.org/10.3390/ijms19051354.

Choate, Keith A., Yin Lu, Jing Zhou, Murim Choi, Peter M. Elias, Anita Farhi, Carol Nelson-Williams, et al. 2010. “Mitotic Recombination in Patients with Ichthyosis Causes Reversion of Dominant Mutations in KRT10.” *Science* 330 (6000): 94–97. https://doi.org/10.1126/science.1192280.

Common, J E A. 2004. “Further Evidence for Heterozygote Advantage of GJB2 Deafness Mutations: A Link with Cell Survival.” *Journal of Medical Genetics* 41 (7): 573–75. https://doi.org/10.1136/jmg.2003.017632.

Courtois, G, and T D Gilmore. 2006. “Mutations in the NF-KB Signaling Pathway: Implications for Human Disease.” *Oncogene* 25 (51): 6831–43. https://doi.org/10.1038/sj.onc.1209939.

Crespin, S., M. Bacchetta, J. Bou Saab, P. Tantilipikorn, J. Bellec, T. Dudez, T.H. Nguyen, et al. 2014. “Cx26 Regulates Proliferation of Repairing Basal Airway Epithelial Cells.” *The International Journal of Biochemistry & Cell Biology* 52 (July): 152–60. https://doi.org/10.1016/j.biocel.2014.02.010.

Czyz, Christianna Marie, Paul Werner Kunth, Florian Gruber, Christopher Kremslehner, Christoph Matthias Hammers, and Jennifer Elisabeth Hundt. 2023. “Requisite Instruments for the Establishment of Three-Dimensional Epidermal Human Skin Equivalents—A Methods Review.” *Experimental Dermatology*. John Wiley and Sons Inc. https://doi.org/10.1111/exd.14911.

Dalamón, Viviana Karina, Paula Buonfiglio, Margarita Larralde, Patricio Craig, Vanesa Lotersztein, Keith Choate, Norma Pallares, Vicente Diamante, and Ana Belén Elgoyhen. 2016. “Connexin 26 (GJB2) Mutation in an Argentinean Patient with Keratitis-Ichthyosis-Deafness (KID) Syndrome: A Case Report.” *BMC Medical Genetics* 17 (1). https://doi.org/10.1186/S12881-016-0298-Y.

Djalilian, Ali R., David McGaughey, Satyakam Patel, Young Seo Eun, Chenghua Yang, Jun Cheng, Melanija Tomic, Satrajit Sinha, Akemi Ishida-Yamamoto, and Julia A. Segre. 2006. “Connexin 26 Regulates Epidermal Barrier and Wound Remodeling and Promotes Psoriasiform Response.” *Journal of Clinical Investigation* 116 (5): 1243. https://doi.org/10.1172/JCI27186.

Donahue, Henry J., Roy W. Qu, and Damian C. Genetos. 2018. “Joint Diseases: From Connexins to Gap Junctions.” *Nature Reviews Rheumatology* 14 (1): 42–51. https://doi.org/10.1038/nrrheum.2017.204.

Dutta, J, Y Fan, N Gupta, G Fan, and C Gélinas. 2006. “Current Insights into the Regulation of Programmed Cell Death by NF-KB.” *Oncogene* 25 (51): 6800–6816. https://doi.org/10.1038/sj.onc.1209938.

Espín-Palazón, Raquel, and David Traver. 2016. “The NF-KB Family: Key Players during Embryonic Development and HSC Emergence.” *Experimental Hematology* 44 (7): 519–27. https://doi.org/10.1016/j.exphem.2016.03.010.

Faniku, Chrysovalantou, Catherine S Wright, and Patricia E Martin. 2015. “Connexins and Pannexins in the Integumentary System: The Skin and Appendages.” *Cellular and Molecular Life Sciences*. Birkhauser Verlag AG. https://doi.org/10.1007/s00018-015-1969-0.

Fischer, Martin, Chi v. Dang, and James A. DeCaprio. 2018. “Control of Cell Division.” In *Hematology*, 176–85. Elsevier. https://doi.org/10.1016/B978-0-323-35762-3.00017-2.

Fuchs, Elaine. 2008. “Skin Stem Cells: Rising to the Surface.” *Journal of Cell Biology*. https://doi.org/10.1083/jcb.200708185.

Fullard, Nicola, Anna Moles, Steven O’Reilly, Jacob M. van Laar, David Faini, Julie Diboll, Nick J. Reynolds, Derek A. Mann, Julia Reichelt, and Fiona Oakley. 2013. “The C-Rel Subunit of NF-KB Regulates Epidermal Homeostasis and Promotes Skin Fibrosis in Mice.” *The American Journal of Pathology* 182 (6): 2109–20. https://doi.org/10.1016/j.ajpath.2013.02.016.

García, Isaac E., Felicitas Bosen, Paula Mujica, Amaury Pupo, Carolina Flores-Muñoz, Oscar Jara, Carlos González, Klaus Willecke, and Agustín D. Martínez. 2016. “From Hyperactive Connexin26 Hemichannels to Impairments in Epidermal Calcium Gradient and Permeability Barrier in the Keratitis-Ichthyosis-Deafness Syndrome.” *Journal of Investigative Dermatology* 136 (3): 574–83. https://doi.org/10.1016/j.jid.2015.11.017.

García, Isaac E., Jaime Maripillán, Oscar Jara, Ricardo Ceriani, Angelina Palacios-Muñoz, Jayalakshmi Ramachandran, Pablo Olivero, et al. 2015. “Keratitis-Ichthyosis-Deafness Syndrome-Associated Cx26 Mutants Produce Nonfunctional Gap Junctions but Hyperactive Hemichannels When Co-Expressed With Wild Type Cx43.” *Journal of Investigative Dermatology* 135 (5): 1338–47. https://doi.org/10.1038/JID.2015.20.

García-Vega, Laura, Erin M O’Shaughnessy, Afnan Jan, Chris Bartholomew, and Patricia E Martin. 2019. “Connexin 26 and 43 Play a Role in Regulating Proinflammatory Events in the Epidermis.” *Journal of Cellular Physiology* 234 (9): 15594–606. https://doi.org/10.1002/jcp.28206.

García-Vega, Laura, Erin M O’Shaughnessy, Ahmad Albuloushi, and Patricia E Martin. 2021. “Connexins and the Epithelial Tissue Barrier: A Focus on Connexin 26.” *Biology* 10 (1): 59. https://doi.org/10.3390/biology10010059.

Geel, M. van, M.A.M. van Steensel, W. Kuster, H.C. Hennies, R. Happle, P.M. Steijlen, and A. Konig. 2002. “HID and KID Syndromes Are Associated with the Same Connexin 26 Mutation.” *British Journal of Dermatology* 146 (6): 938–42. https://doi.org/10.1046/j.1365-2133.2002.04893.x.

Gerido, Dwan A, Adam M Derosa, Gabriele Richard, and Thomas W White. 2007. “Aberrant Hemichannel Properties of Cx26 Mutations Causing Skin Disease and Deafness.” *Am J Physiol Cell Physiol* 293: 337–45. https://doi.org/10.1152/ajpcell.00626.2006.

Goliger, J A, and D L Paul. 1995. “Wounding Alters Epidermal Connexin Expression and Gap Junction-Mediated Intercellular Communication.” *Molecular Biology of the Cell* 6 (11): 1491–1501. https://doi.org/10.1091/mbc.6.11.1491.

Grinberg-Bleyer, Yenkel, Teruki Dainichi, Hyunju Oh, Nicole Heise, Ulf Klein, Roland M. Schmid, Matthew S. Hayden, and Sankar Ghosh. 2015. “Cutting Edge: NF-KB P65 and c-Rel Control Epidermal Development and Immune Homeostasis in the Skin.” *The Journal of Immunology* 194 (6): 2472–76. https://doi.org/10.4049/jimmunol.1402608.

Gugasyan, Raffi, Anne Voss, George Varigos, Tim Thomas, Raelene J. Grumont, Pritinder Kaur, George Grigoriadis, and Steve Gerondakis. 2004. “The Transcription Factors C-Rel and RelA Control Epidermal Development and Homeostasis in Embryonic and Adult Skin via Distinct Mechanisms.” *Molecular and Cellular Biology* 24 (13): 5733–45. https://doi.org/10.1128/MCB.24.13.5733-5745.2004.

Guo, Qing, Yizi Jin, Xinyu Chen, Xiaomin Ye, Xin Shen, Mingxi Lin, Cheng Zeng, Teng Zhou, and Jian Zhang. 2024. “NF-KB in Biology and Targeted Therapy: New Insights and Translational Implications.” *Signal Transduction and Targeted Therapy* 9 (1): 53. https://doi.org/10.1038/s41392-024-01757-9.

Hayden, Matthew S, A P West, and Sankar Ghosh. 2006. “NF-KB and the Immune Response.” *Oncogene* 25 (51): 6758–80. https://doi.org/10.1038/sj.onc.1209943.

Hayden, Matthew S, and Sankar Ghosh. 2011. “NF-KB in Immunobiology.” *Cell Research* 21 (2): 223–44. https://doi.org/10.1038/cr.2011.13.

Hervé, Jean-Claude, Nicolas Bourmeyster, Denis Sarrouilhe, and Heather S. Duffy. 2007. “Gap Junctional Complexes: From Partners to Functions.” *Progress in Biophysics and Molecular Biology* 94 (1–2): 29–65. https://doi.org/10.1016/j.pbiomolbio.2007.03.010.

Hu, Yinling, Véronique Baud, Mireille Delhase, Peilin Zhang, Thomas Deerinck, Mark Ellisman, Randall Johnson, and Michael Karin. 1999. “Abnormal Morphogenesis But Intact IKK Activation in Mice Lacking the IKKα Subunit of IκB Kinase.” *Science* 284 (5412): 316–20. https://doi.org/10.1126/science.284.5412.316.

Jonard, Laurence, Delphine Feldmann, Christophe Parsy, Sylvie Freitag, Martine Sinico, Céleste Koval, Mhamed Grati, et al. 2008. “A Familial Case of Keratitis-Ichthyosis-Deafness (KID) Syndrome with the GJB2 Mutation G45E.” *European Journal of Medical Genetics* 51 (1): 35–43. https://doi.org/10.1016/J.EJMG.2007.09.005.

Kasibhatla, Shailaja, Laurent Genestier, and Douglas R. Green. 1999. “Regulation of Fas-Ligand Expression during Activation-Induced Cell Death in T Lymphocytes via Nuclear Factor KB.” *Journal of Biological Chemistry* 274 (2): 987–92. https://doi.org/10.1074/jbc.274.2.987.

Labarthe, Marie Pierre, Domenico Bosco, Jean Hilaire Saurat, Paolo Meda, and Denis Salomon. 1998. “Upregulation of Connexin 26 between Keratinocytes of Psoriatic Lesions.” *Journal of Investigative Dermatology* 111 (1): 72–76. https://doi.org/10.1046/j.1523-1747.1998.00248.x.

Laird, Dale W., and Paul D. Lampe. 2018. “Therapeutic Strategies Targeting Connexins.” *Nature Reviews. Drug Discovery* 17 (12): 905. https://doi.org/10.1038/NRD.2018.138.

Laird, Dale W., and Paul D. Lampe. 2022. “Cellular Mechanisms Of Connexin-Based Inherited Diseases.” *Trends in Cell Biology* 32 (1): 58. https://doi.org/10.1016/J.TCB.2021.07.007.

Ledoux, Adeline C., and Neil D. Perkins. 2014. “NF-KB and the Cell Cycle.” *Biochemical Society Transactions* 42 (1): 76–81. https://doi.org/10.1042/BST20130156.

Lee, Eric G., David L. Boone, Sophia Chai, Shon L. Libby, Marcia Chien, James P. Lodolce, and Averil Ma. 2000. “Failure to Regulate TNF-Induced NF-KB and Cell Death Responses in A20-Deficient Mice.” *Science* 289 (5488): 2350–54. https://doi.org/10.1126/science.289.5488.2350.

Lee, Hyun-Ji, and Miri Kim. 2022. “Skin Barrier Function and the Microbiome.” *International Journal of Molecular Sciences* 23 (21): 13071. https://doi.org/10.3390/ijms232113071.

Lee, Jack R., and Thomas W. White. 2009. “Connexin-26 Mutations in Deafness and Skin Disease.” *Expert Reviews in Molecular Medicine* 11 (December). https://doi.org/10.1017/S1462399409001276.

Lee, Seung-Chul, Jee-Bum Lee, Jung-Pio Kook, Jae-Jung Seo, Young Pio Kim, Kwang-Il Nam, and Sung-Sik Park. 1999. “Expression of Differentiation Markers During Fetal Skin Development in Humans: Immunohistochemical Studies on the Precursor Proteins Forming the Cornified Cell Envelope.” *Journal of Investigative Dermatology* 112 (6): 882–86. https://doi.org/10.1046/j.1523-1747.1999.00602.x.

Li, Q., Q. Lu, J. Y. Hwang, D. Buscher, K.-F. Lee, J. C. Izpisua-Belmonte, and I. M. Verma. 1999. “IKK1-Deficient Mice Exhibit Abnormal Development of Skin and Skeleton.” *Genes & Development* 13 (10): 1322–28. https://doi.org/10.1101/gad.13.10.1322.

Lilly, Evelyn, Caterina Sellitto, Leonard M. Milstone, and Thomas W. White. 2016. “Connexin Channels in Congenital Skin Disorders.” *Seminars in Cell and Developmental Biology*. Academic Press. https://doi.org/10.1016/j.semcdb.2015.11.018.

Lilly, Evelyn, Michael Strickler, Leonard M. Milstone, and Christopher G. Bunick. 2019. “Alterations in Connexin 26 Protein Structure from Lethal Keratitis-Ichthyosis-Deafness Syndrome Mutations A88V and G45E.” *Journal of Dermatological Science* 95 (3): 119–22. https://doi.org/10.1016/j.jdermsci.2019.07.002.

Lippens, Saskia, Esther Hoste, Peter Vandenabeele, Patrizia Agostinis, and Wim Declercq. 2009. “Cell Death in the Skin.” *Apoptosis* 14 (4): 549–69. https://doi.org/10.1007/s10495-009-0324-z.

Lizzul, Paul F., Abhishek Aphale, Rama Malaviya, Yvonne Sun, Salman Masud, Viktor Dombrovskiy, and Alice B. Gottlieb. 2005. “Differential Expression of Phosphorylated NF-KB/RelA in Normal and Psoriatic Epidermis and Downregulation of NF-KB in Response to Treatment with Etanercept.” *Journal of Investigative Dermatology* 124 (6): 1275–83. https://doi.org/10.1111/j.0022-202X.2005.23735.x.

Loiselle, Alayna E., Jean X. Jiang, and Henry J. Donahue. 2013. “Gap Junction and Hemichannel Functions in Osteocytes.” *Bone* 54 (2): 205–12. https://doi.org/10.1016/j.bone.2012.08.132.

Lopez-Pajares, Vanessa, Karen Yan, Brian J. Zarnegar, Katherine L. Jameson, and Paul A. Khavari. 2013. “Genetic Pathways in Disorders of Epidermal Differentiation.” *Trends in Genetics* 29 (1): 31–40. https://doi.org/10.1016/j.tig.2012.10.005.

Lorenz, Verena Natalie, Michael P. Schön, and Cornelia S. Seitz. 2015. “The C-Rel Subunit of NF-KB Is a Crucial Regulator of Phenotype and Motility of HaCaT Keratinocytes.” *Archives of Dermatological Research* 307 (6): 523–30. https://doi.org/10.1007/s00403-015-1562-2.

Lucke, Tom, Rukhsana Choudhry, Russell Thom, Inger Sofie Selmer, A. David Burden, and Malcolm B. Hodgins. 1999. “Upregulation of Connexin 26 Is a Feature of Keratinocyte Differentiation in Hyperproliferative Epidermis, Vaginal Epithelium, and Buccal Epithelium.” *Journal of Investigative Dermatology* 112 (3): 354–61. https://doi.org/10.1046/j.1523-1747.1999.00512.x.

Man, Y. K. Stella, Caroline Trolove, Daniel Tattersall, Anna C. Thomas, Annie Papakonstantinopoulou, Drashnika Patel, Claire Scott, et al. 2007. “A Deafness-Associated Mutant Human Connexin 26 Improves the Epithelial Barrier In Vitro.” *Journal of Membrane Biology* 218 (1–3): 29–37. https://doi.org/10.1007/s00232-007-9025-0.

Martin, Patricia E, Jennifer A Easton, Malcolm B Hodgins, and Catherine S Wright. 2014. “Connexins: Sensors of Epidermal Integrity That Are Therapeutic Targets.” In *FEBS Letters*, 588:1304–14. Elsevier. https://doi.org/10.1016/j.febslet.2014.02.048.

Martin, Patricia E.M., and Maurice van Steensel. 2015. “Connexins and Skin Disease: Insights into the Role of Beta Connexins in Skin Homeostasis.” *Cell and Tissue Research* 360 (3): 645–58. https://doi.org/10.1007/S00441-014-2094-3/TABLES/2.

Matsui, Ken, Alan Fine, Bangmin Zhu, Ann Marshak-Rothstein, and Shyr-Te Ju. 1998. “Identification of Two NF-KB Sites in Mouse CD95 Ligand (Fas Ligand) Promoter: Functional Analysis in T Cell Hybridoma.” *The Journal of Immunology* 161 (7): 3469–73. https://doi.org/10.4049/jimmunol.161.7.3469.

Mazereeuw-Hautier, J., E. Bitoun, J. Chevrant-Breton, S.Y.K. Man, C. Bodemer, C. Prins, C. Antille, et al. 2007. “Keratitis-Ichthyosis-Deafness Syndrome: Disease Expression and Spectrum of Connexin 26 (GJB2) Mutations in 14 Patients.” *British Journal of Dermatology* 156 (5): 1015–19. https://doi.org/10.1111/j.1365-2133.2007.07806.x.

Meigh, Louise, Naveed Hussain, Daniel K Mulkey, and Nicholas Dale. 2014. “Connexin26 Hemichannels with a Mutation That Causes KID Syndrome in Humans Lack Sensitivity to CO2.” *ELife* 3 (November). https://doi.org/10.7554/eLife.04249.

Menon, Gopinathan K., Gary W. Cleary, and Majella E. Lane. 2012. “The Structure and Function of the Stratum Corneum.” *International Journal of Pharmaceutics* 435 (1): 3–9. https://doi.org/10.1016/j.ijpharm.2012.06.005.

Mese, Gulistan, Caterina Sellitto, Leping Li, Hong Zhan Wang, Virginijus Valiunas, Gabriele Richard, Peter R. Brink, and Thomas W. White. 2011. “The Cx26-G45E Mutation Displays Increased Hemichannel Activity in a Mouse Model of the Lethal Form of Keratitis-Ichthyosis-Deafness Syndrome.” *Molecular Biology of the Cell* 22 (24): 4776. https://doi.org/10.1091/MBC.E11-09-0778.

Mese, Gülistan, Virginijus Valiunas, Peter R Brink, and Thomas W White. 2008. “Connexin26 Deafness Associated Mutations Show Altered Permeability to Large Cationic Molecules.” *Am J Physiol Cell Physiol* 295 (4): 966–74. https://doi.org/10.1152/ajpcell.00008.2008.

Mhaske, Pallavi v., Noah A. Levit, Leping Li, Hong Zhan Wang, Jack R. Lee, Zunaira Shuja, Peter R. Brink, and Thomas W. White. 2013. “The Human Cx26-D50A and Cx26-A88V Mutations Causing Keratitis-Ichthyosis-Deafness Syndrome Display Increased Hemichannel Activity.” *American Journal of Physiology - Cell Physiology* 304 (12): C1150. https://doi.org/10.1152/AJPCELL.00374.2012.

Mori, Ryoichi, Kieran T. Power, Chiuhui Mary Wang, Paul Martin, and David L. Becker. 2006. “Acute Downregulation of Connexin43 at Wound Sites Leads to a Reduced Inflammatory Reponse, Enhanced Keratinocyte Proliferation and Wound Fibroblast Migration.” *Journal of Cell Science* 119 (24): 5193–5203. https://doi.org/10.1242/jcs.03320.

Ng, Dean C., Simira Shafaee, David Lee, and Daniel D. Bikle. 2000. “Requirement of an AP-1 Site in the Calcium Response Region of the Involucrin Promoter.” *Journal of Biological Chemistry* 275 (31): 24080–88. https://doi.org/10.1074/jbc.M002508200.

Nielsen, Morten Schak, Lene Nygaard Axelsen, Paul L. Sorgen, Vandana Verma, Mario Delmar, and Niels-Henrik Holstein-Rathlou. 2012. “Gap Junctions.” In *Comprehensive Physiology*, 1981–2035. Wiley. https://doi.org/10.1002/cphy.c110051.

Niessen, Heiner, Hartmann Harz, Peter Bedner, Karsten Krämer, and Klaus Willecke. 2000. “Selective Permeability of Different Connexin Channels to the Second Messenger Inositol 1,4,5-Trisphosphate.” *Journal of Cell Science* 113 (8): 1365–72. https://doi.org/10.1242/jcs.113.8.1365.

Nyquist, Gurston G., Christina Mumm, Renee Grau, A. Neil Crowson, Daniel L. Shurman, Paul Benedetto, Pamela Allen, et al. 2007. “Malignant Proliferating Pilar Tumors Arising in KID Syndrome: A Report of Two Patients.” *American Journal of Medical Genetics Part A* 143A (7): 734–41. https://doi.org/10.1002/ajmg.a.31635.

Oeckinghaus, A., and S. Ghosh. 2009. “The NF- B Family of Transcription Factors and Its Regulation.” *Cold Spring Harbor Perspectives in Biology* 1 (4): a000034–a000034. https://doi.org/10.1101/cshperspect.a000034.

Pahl, Heike L. 1999. “Activators and Target Genes of Rel/NF-KB Transcription Factors.” *Oncogene* 18 (49): 6853–66. https://doi.org/10.1038/sj.onc.1203239.

Pease, Louise I, James Wordsworth, and Daryl P. Shanley. 2022. “Transcriptomic and Epigenetic Assessment of Ageing Female Skin and Fibroblasts Identifies Age Related Reduced Oxidative Phosphorylation Is Exacerbated by Smoking.” *BioRxiv*.

Peres, Chiara, Caterina Sellitto, Chiara Nardin, Sabrina Putti, Tiziana Orsini, Chiara di Pietro, Daniela Marazziti, et al. 2023. “Antibody Gene Transfer Treatment Drastically Improves Epidermal Pathology in a Keratitis Ichthyosis Deafness Syndrome Model Using Male Mice.” *EBioMedicine* 89 (March): 104453. https://doi.org/10.1016/j.ebiom.2023.104453.

Perugini, Richard A., Theodore P. McDade, Frank J. Vittimberga, Andrew J. Duffy, and Mark P. Callery. 2000. “Sodium Salicylate Inhibits Proliferation and Induces G1 Cell Cycle Arrest in Human Pancreatic Cancer Cell Lines.” *Journal of Gastrointestinal Surgery* 4 (1): 24–33. https://doi.org/10.1016/S1091-255X(00)80029-3.

Posukh, Olga L., Ekaterina A. Maslova, Valeriia Yu Danilchenko, Marina v. Zytsar, and Konstantin E. Orishchenko. 2023. “Functional Consequences of Pathogenic Variants of the GJB2 Gene (Cx26) Localized in Different Cx26 Domains.” *Biomolecules* 13 (10). https://doi.org/10.3390/BIOM13101521.

Press, Eric R., Qing Shao, John J. Kelly, Katrina Chin, Anton Alaga, and Dale W. Laird. 2017. “Induction of Cell Death and Gain-of-Function Properties of Connexin26 Mutants Predict Severity of Skin Disorders and Hearing Loss.” *Journal of Biological Chemistry* 292 (23): 9721–32. https://doi.org/10.1074/jbc.M116.770917.

Qiu, Yue, Jianglin Zheng, Sen Chen, and Yu Sun. 2022. “Connexin Mutations and Hereditary Diseases.” *International Journal of Molecular Sciences* 23 (8): 4255. https://doi.org/10.3390/ijms23084255.

Richard, Gabriele, Nkecha Brown, Akemi Ishida-Yamamoto, and Alfons Krol. 2004. "Expanding the Phenotypic Spectrum of Cx26 Disorders: Bart-Pumphrey Syndrome Is Caused by a Novel Missense Mutation in GJB2." *Journal of Investigative Dermatology* 123 (5): 856–63. https://doi.org/10.1111/j.0022-202X.2004.23470.x.

Richard, Gabriele, Fatima Rouan, Colin E. Willoughby, Nkecha Brown, Pil Chung, Markku Ryynänen, Ethylin Wang Jabs, et al. 2002. "Missense Mutations in GJB2 Encoding Connexin-26 Cause the Ectodermal Dysplasia Keratitis-Ichthyosis-Deafness Syndrome." *American Journal of Human Genetics* 70 (5): 1341. https://doi.org/10.1086/339986.

Rivas, Miriam v, Erich D Jarvis, S Morisaki, H Carbonaro, A. B. Gottlieb, and J. G. Krueger. 1997. "Identification of Aberrantly Regulated Genes Diseased Skin Using the CDNA Differential Display Technique." *Journal of Investigative Dermatology* 108 (2): 188–94. https://doi.org/10.1111/1523-1747.ep12334217.

Robert, Caroline, and Thomas S. Kupper. 1999. "Inflammatory Skin Diseases, T Cells, and Immune Surveillance." *New England Journal of Medicine* 341 (24): 1817–28. https://doi.org/10.1056/NEJM199912093412407.

Rousselle, Patricia, Edgar Gentilhomme, and Yves Neveux. 2017. "Markers of Epidermal Proliferation and Differentiation." In *Agache's Measuring the Skin*, 407–15. Cham: Springer International Publishing. https://doi.org/10.1007/978-3-319-32383-1_37.

Sanchez, Helmuth A., and Vytas K. Verselis. 2014. "Aberrant Cx26 Hemichannels and Keratitis-Ichthyosis-Deafness Syndrome: Insights into Syndromic Hearing Loss." *Frontiers in Cellular Neuroscience*. Frontiers Media S.A. https://doi.org/10.3389/fncel.2014.00354.

Schmidt-Supprian, Marc, Wilhelm Bloch, Gilles Courtois, Klaus Addicks, Alain Israël, Klaus Rajewsky, and Manolis Pasparakis. 2000. "NEMO/IKKγ-Deficient Mice Model Incontinentia Pigmenti." *Molecular Cell* 5 (6): 981–92. https://doi.org/10.1016/S1097-2765(00)80263-4.

Schütz, Melanie, Tanja Auth, Anna Gehrt, Felicitas Bosen, Inken Körber, Nicola Strenzke, Tobias Moser, and Klaus Willecke. 2011. “The Connexin26 S17F Mouse Mutant Represents a Model for the Human Hereditary Keratitis–Ichthyosis–Deafness Syndrome.” *Human Molecular Genetics* 20 (1): 28–39. https://doi.org/10.1093/HMG/DDQ429.

Scott, Claire A., Daniel Tattersall, Edel A. O’Toole, and David P. Kelsell. 2012. “Connexins in Epidermal Homeostasis and Skin Disease.” *Biochimica et Biophysica Acta - Biomembranes*. https://doi.org/10.1016/j.bbamem.2011.09.004.

Seishima, Mariko, Mari Nojiri, Chikako Esaki, Kozo Yoneda, Yuzuru Eto, and Yasuo Kitajima. 1999. “Activin A Induces Terminal Differentiation of Cultured Human Keratinocytes.” *Journal of Investigative Dermatology* 112 (4): 432–36. https://doi.org/10.1046/j.1523-1747.1999.00558.x.

Seitz, Cornelia S., Qun Lin, Helen Deng, and Paul A. Khavari. 1998. “Alterations in NF-KB Function in Transgenic Epithelial Tissue Demonstrate a Growth Inhibitory Role for NF-KB.” *Proceedings of the National Academy of Sciences* 95 (5): 2307–12. https://doi.org/10.1073/pnas.95.5.2307.

Sen, Ranjan, and David Baltimore. 1986. “Multiple Nuclear Factors Interact with the Immunoglobulin Enhancer Sequences.” *Cell* 46 (5): 705–16. https://doi.org/10.1016/0092-8674(86)90346-6.

Serasanambati, Mamatha, and Shanmuga Reddy Chilakapati. 2016. “Function of Nuclear Factor Kappa B (NF-KB) in Human Diseases- A Review.” *South Indian Journal of Biological Sciences* 2 (4): 368–87. https://doi.org/10.22205/SIJBS/2016/V2/I4/103443.

Shen, Yitong, Anne P. R. Boulton, Robert L. Yellon, and Matthew C. Cook. 2023. “Skin Manifestations of Inborn Errors of NF-KB.” *Frontiers in Pediatrics* 10 (January). https://doi.org/10.3389/fped.2022.1098426.

Sotiropoulou, Panagiota A., and Cedric Blanpain. 2012. “Development and Homeostasis of the Skin Epidermis.” *Cold Spring Harbor Perspectives in Biology* 4 (7): 1–9. https://doi.org/10.1101/CSHPERSPECT.A008383.

Srinivas, Miduturu, Vytas K. Verselis, and Thomas W. White. 2018. “Human Diseases Associated with Connexin Mutations.” *Biochimica et Biophysica Acta (BBA) - Biomembranes* 1860 (1): 192–201. https://doi.org/10.1016/j.bbamem.2017.04.024.

Stong, Benjamin C., Qing Chang, Shoeb Ahmad, and Xi Lin. 2006. “A Novel Mechanism for Connexin 26 Mutation Linked Deafness: Cell Death Caused by Leaky Gap Junction Hemichannels.” *The Laryngoscope* 116 (12): 2205–10. https://doi.org/10.1097/01.MLG.0000241944.77192.D2.

Sun, Minqiong, Yuan Li, Jing Qian, Siwei Ding, Mingyu Sun, Bowen Tan, and Ye Zhao. 2021. “Connexin26 Modulates the Radiosensitivity of Cutaneous Squamous Cell Carcinoma by Regulating the Activation of the MAPK/NF-KB Signaling Pathway.” *Frontiers in Cell and Developmental Biology* 9 (July). https://doi.org/10.3389/fcell.2021.672571.

Sur, Inderpreet, Maria Ulvmar, and Rune Toftgård. 2008. “The Two-Faced NF-KB in the Skin.” *International Reviews of Immunology* 27 (4): 205–23. https://doi.org/10.1080/08830180802130319.

Takao, J., T. Yudate, A. Das, S. Shikano, M. Bonkobara, K. Ariizumi, and P.D. Cruz. 2003. “Expression of NF-KappaB in Epidermis and the Relationship between NF-KappaB Activation and Inhibition of Keratinocyte Growth.” *British Journal of Dermatology* 148 (4): 680–88. https://doi.org/10.1046/j.1365-2133.2003.05285.x.

Taki, T., T. Takeichi, K. Sugiura, and M. Akiyama. 2018. “Roles of Aberrant Hemichannel Activities Due to Mutant Connexin26 in the Pathogenesis of KID Syndrome.” *Scientific Reports* 8 (1). https://doi.org/10.1038/s41598-018-30757-3.

Tanaka, Motoyoshi, and H Barton Grossman. 2004. “Connexin 26 Induces Growth Suppression, Apoptosis and Increased Efficacy of Doxorubicin in Prostate Cancer Cells.” *Oncology Reports* 11 (2): 537–41.

Thomas, Tamsin, Debra Telford, and Dale W. Laird. 2004. “Functional Domain Mapping and Selective Trans-Dominant Effects Exhibited by Cx26 Disease-Causing Mutations.” *Journal of Biological Chemistry* 279 (18): 19157–68. https://doi.org/10.1074/jbc.M314117200.

Wang, Yujia, Lian Wang, Xiang Wen, Dan Hao, Nan Zhang, Gu He, and Xian Jiang. 2019. “NF-KB Signaling in Skin Aging.” *Mechanisms of Ageing and Development* 184 (December): 111160. https://doi.org/10.1016/j.mad.2019.111160.

Weber, Paul A., Hou-Chien Chang, Kris E. Spaeth, Johannes M. Nitsche, and Bruce J. Nicholson. 2004. “The Permeability of Gap Junction Channels to Probes of Different Size Is Dependent on Connexin Composition and Permeant-Pore Affinities.” *Biophysical Journal* 87 (2): 958–73. https://doi.org/10.1529/biophysj.103.036350.

Weih, Falk, Stephen K. Durham, Debra S. Barton, William C. Sha, David Baltimore, and Rodrigo Bravo. 1997. “P50–NF-KB Complexes Partially Compensate for the Absence of RelB: Severely Increased Pathology in P50−/− RelB−/− Double-Knockout Mice.” *The Journal of Experimental Medicine* 185 (7): 1359–70. https://doi.org/10.1084/jem.185.7.1359.

Wong, Daniel, Ana Teixeira, Spyros Oikonomopoulos, Peter Humburg, Imtiaz Lone, David Saliba, Trevor Siggers, et al. 2011. “Extensive Characterization of NF-KB Binding Uncovers Non-Canonical Motifs and Advances the Interpretation of Genetic Functional Traits.” *Genome Biology* 12 (7): R70. https://doi.org/10.1186/gb-2011-12-7-r70.

Wright, John Timothy, Mary Fete, Holm Schneider, Madelaine Zinser, Maranke I. Koster, Angus J. Clarke, Smail Hadj-Rabia, et al. 2019. “Ectodermal Dysplasias: Classification and Organization by Phenotype, Genotype and Molecular Pathway.” *American Journal of Medical Genetics Part A* 179 (3): 442–47. https://doi.org/10.1002/ajmg.a.61045.

Yasarbas, S. Suheda, Ece Inal, M. Azra Yildirim, Sandrine Dubrac, Jérôme Lamartine, and Gulistan Mese. 2024. “Connexins in Epidermal Health and Diseases: Insights into Their Mutations, Implications, and Therapeutic Solutions.” *Frontiers in Physiology* 15 (May). https://doi.org/10.3389/fphys.2024.1346971.

Yotsumoto, S., T. Hashiguchi, X. Chen, N. Ohtake, A. Tomitaka, H. Akamatsu, K. Matsunaga, et al. 2003. “Novel Mutations in GJB2 Encoding Connexin-26 in Japanese Patients with Keratitis-Ichthyosis-Deafness Syndrome.” *British Journal of Dermatology* 148 (4): 649–53. https://doi.org/10.1046/j.1365-2133.2003.05245.x.

Yousef, Hani, Mandy Alhajj, and Sandeep Sharma. 2022. “Anatomy, Skin (Integument), Epidermis.” In: StatPearls [Internet]. Treasure Island (FL): StatPearls Publishing. November 14, 2022. https://www.ncbi.nlm.nih.gov/books/NBK470464/.

Zhang, Qian, Michael J. Lenardo, and David Baltimore. 2017. “30 Years of NF-KB: A Blossoming of Relevance to Human Pathobiology.” *Cell* 168 (1–2): 37–57. https://doi.org/10.1016/j.cell.2016.12.012.

Zhang, Xiao-Fei, and Xiaofeng Cui. 2017. “Connexin 43: Key Roles in the Skin.” *Biomedical Reports* 6 (6): 605–11. https://doi.org/10.3892/br.2017.903.